

Adaptive Fuzzy Control for Coordinated Multiple Robots with Constraint Using Impedance Learning

Linghuan Kong, Wei He, *Senior Member, IEEE*, Chenguang Yang, *Senior Member, IEEE*, Zhijun Li, *Senior Member, IEEE*, and Changyin Sun

Abstract—In this paper, we investigate fuzzy neural network (FNN) control using impedance learning for coordinated multiple constrained robots carrying a common object in the presence of the unknown robotic dynamics and the unknown environment with which the robot comes into contact. Firstly, a FNN learning algorithm is developed to identify the unknown plant model. Secondly, impedance learning is introduced to regulate the control input in order to improve the environment-robot interaction, and the robot can track the desired trajectory generated by impedance learning. Thirdly, in light of the condition requiring the robot to move in a finite space or to move at a limited velocity in a finite space, the algorithm based on the position constraint and the velocity constraint are proposed, respectively. To guarantee the position constraint and the velocity constraint, Integral Barrier Lyapunov function (IBLF) is introduced to avoid the violation of the constraint. According to Lyapunov's stability theory, it can be proved that the tracking errors are uniformly bounded ultimately. At last, Some simulation examples are carried out to verify the effectiveness of the designed control.

Index Terms—Fuzzy Systems, Neural Networks, Multiple Robots, Adaptive Control, Time-varying Constraint, Impedance Learning

I. INTRODUCTION

IN recent years, robots have been widely used in medicine [1]–[3], aerospace [4], [5] and marine vessel [6], [7], etc. As the complexity of the task and the demand of control accuracy increase, single robot hardly meet the mission requirement. Multiple robots can complete some tasks which are impossible for a robot. When an object is carried, multiple robots would present a large advantage over a robot in carry velocity and object weight. For example, in tool using tasks such as screwing, distribution of motions and forces required by the tasks between the multiple robot arms greatly reduces

Manuscript received November 3, 2017; revised March 16, 2018; accepted May 3, 2018. This work was supported in part by the National Natural Science Foundation of China under Grant 61522302, Grant 61573147, Grant 61625303, Grant 61751310, and Grant U1713209, in part by the National Basic Research Program of China (973 Program) under Grant 2014CB744206, in part by Anhui Science and Technology Major Program under Grant 17030901029, and in part by the Fundamental Research Funds for the China Central Universities of USTB under Grant FRF-BD-17-002A. This paper was recommended by Associate Editor C.-F. Juang. (Corresponding author: *Wei He*.)

L. Kong and W. He are with the School of Automation and Electrical Engineering, University of Science and Technology Beijing, Beijing 100083, China, and also with the Institute of Artificial Intelligence, University of Science and Technology Beijing, Beijing 100083, China. (Email: weihe@ieee.org)

C. Yang was with the Zienkiewicz Centre for Computational Engineering, Swansea University, Swansea SA1 8EN, U.K. He is now with Bristol Robotics Laboratory, University of the West of England, Bristol, BS16 1QY, U.K.

Z. Li is with the Department of Automation, University of Science and Technology of China, Hefei 230026, China.

C. Sun is with School of Automation, Southeast University, Nanjing 210096, China.

the complexity and energy cost of manipulation. Therefore, research on coordinated control of multiple robots would be significant [8]. In robot applications, robot control must be subject to uncertain constraints. The violation of these constraints leads to undesired performances such as performance degradation, hazards or system damages. And the structure of each robot is often different and there exist unmodeled dynamics and unknown parameters, accurate control of such a complicated system is difficult to obtain. However, when working in a limited environment, the robot often comes in contact with the unknown environment which is often difficult to describe in a nonlinear model, and an interaction force develops between the robot and its environment. Therefore, the main difficulty of controlling those systems lies in the fact that, when the robot encounters unknown environments, the interaction force and the position of the robot, must be controlled collaboratively. In this paper, we would analyse coordinated control problems of multiple robots with time-varying constraints in the present of the unknown environment and unmodeled dynamics and design adaptive fuzzy neural network control for coordinated control of multiple robots in a finite task space.

It is well known that adaptive neural networks have a learning capability, and can be considered as a powerful tool to approximate any nonlinear functions to any accuracy in control and applications for nonlinear systems [9]–[16]. The learning capability of neural networks are employed to recognize the unknown plant [17]–[23]. In [24], an intelligent observer which is based on the learning capability of neural networks is designed to observe the unmeasurable states. The approximation property of neural networks is guaranteed only over a compact, and if some parameters are beyond this compact, the learning capability would be reduced [25]. In [26], to tackle this challenge, a robust term is introduced to compensate for the approximation error of neural networks so that it can extend the semiglobal stability by neural networks to global stability. This method has been shown to be effective in tackling the global stability, but it cause the lack of self-learning capability. After that, some research results have incorporated fuzzy techniques to neural network structure in order to obtain global learning capabilities [27]. Furthermore, fuzzy neural networks are hybrid intelligent systems that combine advantages of both fuzzy systems and neural networks. As a result, the combination of the two techniques can not only avoid the lack of interpretability for neural networks but also enhance learning capabilities of fuzzy systems. And this technology can reduce online computation load by using fewer adjustable parameters and be also employed to identify the unknown nonlinear function [28]–[35]. In [36], fuzzy

neural networks are used to identify the unknown plant of an environment-robot system, and the fuzzy algorithm can improve the interaction between the robot and its environment. In [37], fuzzy neural networks are used to approximate the unknown nonlinear plant of nonlinear systems. In [38], an adaptive fuzzy neural network control scheme is proposed for a marine, and the fuzzy policy can ensure that the tracking error converges to an arbitrarily small region near zero in a finite time.

Recently, the tracking control for nonlinear systems is investigated, motivated by the fact that practical systems are subjected to constraint [39] in the form of mechanical structure, safety specifications and physics performance. These constraints include input constraint [40]–[45], output constraint [46]–[48] and full-state constraint [49]–[51]. An appropriate controller sometimes makes the index of a system remain the corresponding constraint region in order to obtain an approximation optimal performance. In [52], it has been proved that *log*-type Barrier Lyapunov functions can guarantee the constraint. In [53], *log*-type Barrier Lyapunov function is introduced to guarantee the full-states remain in the predefined constraint region. However, the above *log*-type Barrier Lyapunov function constraint technique may make the corresponding variables go beyond the constraint region when the size of the vibration is too large or initial values are too large, which may lead to system impairments or even system failures. In [54], Integral Barrier Lyapunov function (IBLF) can compensate the effect of constraint and avoid the violation of states without the requirement of initial values, except that when initial values are demanded to satisfy the constraint. However, *log*-type Barrier Lyapunov function introduced in [52], [53], [55] just constrains error signals, therefore, an additional mapping to the state space is needed. Integral Barrier Lyapunov functions introduced in [56] directly constrain state signals without an additional mapping, and initial states are relaxed to whole constrained space. In [55], *log*-type Barrier Lyapunov functions are used to avoid the violation of the time-varying constraint for a constrained robot. The time-varying constraint is more general than the constant constraint introduced in [52].

Position control methods give adequate performances for an uncertain robot, and only require the robotic end-effector to track a desired trajectory in free space. But, when the robot comes in contact with the environment, it is inevitable that an interaction force would develop between the robot and its environment. Research studies then focus on how to regulate the robot-environment interaction. Hogan first presents impedance control theory to regulate the interaction between the robotic end-effector and the force exerted on the environment. [57] thinks the learning capability can regular the interaction between the robot and its environment. In [58], two impedance control algorithms that generate a desired dynamics of the robot with environment are developed for robotic manipulators. However, the results mentioned in [57]–[59] assume that robot dynamics is known. In [60], adaptive impedance learning control is proposed for a human-robot system in the presence of unknown robotic dynamics.

This paper would handle coordinated control problems of multiple robots with time-varying constraints, in the present

of the unknown environment with which the robot comes into contact. Impedance learning is employed to improve the environment-robot interaction, fuzzy neural networks are constructed to approximate the unknown robotic dynamics, and time-varying constraints guarantee a satisfactory tracking performance by ensuring that the system states remain in a small neighborhood of the reference signal, such that the fuzzy neural network control algorithm is formed. This type of the control algorithm is suitable for the environment-robot interaction control and objection manipulation. This paper is an extended work from the previous works [26], [36]. In [36], only single robot with the constant constraint is considered for the environment-robot interaction without involving coordinated control of multiple robots. But in most situations, multiple robots with the time-varying constraint would present a large advantage over a robot with the constant constraint in the movement velocity and the carried weight. Further, in [26], coordinated control of two robots is investigated without considering the time-varying constraint. Consequently, our work can be considered as the improvement of [26], [36]. Fuzzy neural networks combine advantages of both fuzzy systems and neural networks, and have fewer adjustable parameters and can reduce online computation load. Thus fuzzy neural network control can satisfy the requirement of real-time control better with fewer time consuming.

The main contributions of this paper are summarized as follows: 1) Compared with the conventional Lyapunov functions including *log*-type [55] and *tan*-type [36], integral barrier Lyapunov functions are developed to constrain state signals directly, rather than error signals, with avoiding carrying out an additional mapping to the state space. Therefore, the initial states can be relaxed to whole constrained space. 2) An learning algorithm based on FNN structure is proposed, which needs no previous information of the system. The unknown system plant is approximated by structuring an appropriate FNN structure. 3) The time-varying output constraint and the time-varying full-state constraint are considered, respectively. The time-varying constraint is more general and complicated than constant constraint. Based on the time-varying constraint, the designed algorithm has a wider application range. 4) Impedance learning is introduced to improve the interaction between the robot and the unknown environment.

Notations 1: Let $\lambda_{\min}(\bullet)$ and $\lambda_{\max}(\bullet)$ denote the minimum and maximum eigenvalues of matrix \bullet , respectively. Let $\|\cdot\|$ be the Euclidean norm of a vector. Let $\text{blockdiag}[A_1, A_2, \dots, A_n]$ denote a diagonal block matrix, where $A_i, i = 1, \dots, n$, is a matrix. Let $\text{sgn}(\cdot)$ be a sign function, where

$$\text{sgn}(\cdot) = \begin{cases} 1, & \cdot \geq 0 \\ -1, & \cdot < 0 \end{cases} \quad (1)$$

II. PRELIMINARIES AND PROBLEM FORMULATION

A. System Description

We would investigate an environment-robot interaction system, which includes m robots, the unknown environment, an object and the force sensor located at the object and measuring force exerted by the unknown environment to the robot as Fig. 1 shows. Suppose that there is no information about the

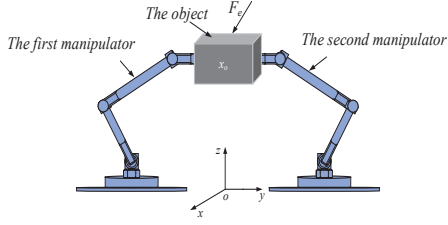


Fig. 1. Coordinated control of two robotic manipulators

environment dynamics and that there exist unmodeled plants and unknown parameters in the robot model. But m robots are demanded to carry an object in a coordinated way in a finite space. Therefore, the main problems are to tackle the unknown dynamics and unknown parameters of the robotic model, the interaction between the robot and its unknown environment, and the time-varying constraint. The kinetic equation of i th manipulator [26] in joint space is expressed as

$$D_i(q_i)\ddot{q}_i + C_i(q_i, \dot{q}_i)\dot{q}_i + G_i(q_i) = \tau_i - J_i^T(q_i)\tau_{ei} \quad (2)$$

$i = 1, \dots, m$

where $q_i \in \mathbb{R}^n$ is the vector of joint variable, $D_i(q_i) \in \mathbb{R}^{n \times n}$ denotes the positive definite joint quality inertia matrix, $C_i(q_i, \dot{q}_i) \in \mathbb{R}^{n \times n}$ denotes the joint Coriolis and centrifugal matrix, $G_i(q_i)$ denotes the joint gravitational forces, $\tau_i \in \mathbb{R}^n$ denotes the control input vector, $J_i(q_i) \in \mathbb{R}^{n \times n}$ denotes the Jacobian matrix, $\tau_{ei} \in \mathbb{R}^n$ denotes the force from the object.

Based on (2), the kinetic equation of m robots is given by

$$D_x(q)\ddot{q} + C_x(q, \dot{q})\dot{q} + G_x(q) = \tau - J^T(q)\tau_e \quad (3)$$

where $q = [q_1^T, \dots, q_m^T]^T \in \mathbb{R}^{mn}$; $\tau = [\tau_1^T, \dots, \tau_m^T]^T \in \mathbb{R}^{mn}$; $\tau_e = [\tau_{e1}^T, \dots, \tau_{em}^T]^T \in \mathbb{R}^{mn}$; $D_x(q) = \text{blockdiag}[D_1(q_1), \dots, D_m(q_m)] \in \mathbb{R}^{mn \times mn}$; $C_x(q, \dot{q}) = \text{blockdiag}[C_1(q_1, \dot{q}_1), \dots, C_m(q_m, \dot{q}_m)] \in \mathbb{R}^{mn \times mn}$; $G_x(q) = [G_1^T(q_1), \dots, G_m^T(q_m)]^T \in \mathbb{R}^{mn}$; $J(q) = \text{blockdiag}[J_1(q_1), \dots, J_m(q_m)] \in \mathbb{R}^{mn \times mn}$.

Let $x_o \in \mathbb{R}^n$ denote the position/orientation vector of the object. The motion of the object is driven by the force vector $\tau_o \in \mathbb{R}^n$ and $\tau_d \in \mathbb{R}^n$ acting on the center of mass the object, where τ_o denotes the resultant force vector from m robots and τ_d denotes the force vector from the unknown environment. The kinetic equation [26] of the object is given by

$$M_o(x_o)\ddot{x}_o + C_o(x_o, \dot{x}_o)\dot{x}_o + G_o(x_o) = \tau_o - \tau_d \quad (4)$$

and $M_o(x_o) \in \mathbb{R}^{n \times n}$ is a symmetric positive definite inertial matrix, $C_o(x_o, \dot{x}_o) \in \mathbb{R}^{n \times n}$ is a corioli and centrifugal matrix, $G_o(x_o) \in \mathbb{R}^n$ is the gravitational force vector. Let $x_i, i = 1, \dots, m$, denote the position/orientations of i th robot's end-effector in the Cartesian space. According to [61], the relationship between x_i and q_i is given by

$$\dot{x}_i = J_i(q_i)\dot{q}_i \quad (5)$$

The relationship [8] between \dot{x}_i and \dot{x}_o is given by

$$\dot{x}_i = J_{io}(x_o)\dot{x}_o \quad (6)$$

where $J_{io}(x_o)$ denotes the Jacobian matrix from the object frame to the i th robot's end-effector. By combining (5) and (6), the relationship between the joint velocity of the i th

manipulator and the velocity of the object is obtained by

$$J_i(q_i)\dot{q}_i = J_{io}(x_o)\dot{x}_o \quad (7)$$

Assume that robots work in a nonsingular region, thus the inverse of the Jacobian matrix $J_i(q_i)$ exists. Considering all the manipulators acting on the object at the same time, yields

$$\dot{q} = J^{-1}(q)J_o(x_o)\dot{x}_o \quad (8)$$

$$\ddot{q} = \frac{d}{dt}(J^{-1}(q)J_o(x_o))\dot{x}_o + J^{-1}(q)J_o(x_o)\ddot{x}_o \quad (9)$$

where $J_o(x_o) = [J_{1o}^T(x_o), \dots, J_{mo}^T(x_o)]^T$. After substituting (8) and (9) into (3) and then adding (4), the kinetic equation of m coordinated multiple robots with object motion (4) in Cartesian space is given by

$$M(q)\ddot{x}_o + C(q, \dot{q})\dot{x}_o + G(q) = F_o - F_e \quad (10)$$

where

$$\begin{aligned} M(q) &= J_o^T(x_o)J^{-T}(q)D_x(q)J^{-1}(q)J_o(x_o) + M_o(x_o) \\ C(q, \dot{q}) &= J_o^T(x_o)J^{-T}(q)D_x(q)\frac{d}{dt}(J^{-1}(q)J_o(x_o)) \\ &\quad + J_o^T(x_o)J^{-T}(q)C_x(q, \dot{q})J^{-1}(q)J_o(x_o) + C_o(x_o, \dot{x}_o) \\ G(q) &= J_o^T(x_o)J^{-T}(q)G_x(q) + G_o(x_o) \\ F_o &= J_o^T(x_o)J^{-T}(q)\tau, \quad F_e = \tau_d \end{aligned}$$

For the convenience, in the subsequent design, M, C, G denote $M(q), C(q, \dot{q}), G(q)$, respectively.

The system state $x_o = [x_{o1}, \dots, x_{on}]^T$ is commanded to satisfy the following constraint

$$|x_{oi}| < k_{ci}, \quad |\dot{x}_{oi}| < k_{di}, \quad i = 1, \dots, n \quad (11)$$

where k_{ci}, k_{di} are positive time-varying functions, given the initial states satisfy $|x_{oi}(0)| < k_{ci}(0), |\dot{x}_{oi}(0)| < k_{di}(0)$. The full-state constraint is denoted as the set $\{x_o \in \mathbb{R}^n \mid |x_{oi}| < k_{ci}, |\dot{x}_{oi}| < k_{di}, i = 1, \dots, n\}$. The output constraint is denoted as the set $\{x_o \in \mathbb{R}^n \mid |x_{oi}| < k_{ci}, i = 1, \dots, n\}$.

In real robotic systems, the object usually suffers from force from environment when moving in task space. The impedance dynamics between F_e and e is given by

$$M_d\ddot{e} + C_d\dot{e} + G_de = F_e \quad (12)$$

where M_d, C_d, G_d are defined by the user. Impedance error e originates from force F_e . Let us define $e = x_d - x_c$, where x_c is the desired trajectory, x_d is the commanded trajectory the users define, which is bounded and twice differentiable. It can be known from (12) that impedance error e is equal to zero if F_e is equal to zero. Substituting $e = x_d - x_c$ into (12), yields

$$M_d\ddot{x}_c + C_d\dot{x}_c + G_dx_c = M_d\ddot{x}_d + C_d\dot{x}_d + G_dx_d - F_e \quad (13)$$

According to (13), the impedance control objective can be achieved. It should be noted that (13) may be interpreted as a simply filter and x_c is obtained online if x_d, M_d, C_d, G_d and the force F_e are given.

B. Fuzzy Neural Networks

A fuzzy system consists of four parts: the knowledge base, the fuzzifier, the fuzzy inference engine working on

fuzzy rules, and the defuzzifier [62]. Consider l fuzzy IF-THEN rules $\mathbb{R}^{(k)}$: If x_1 is A_1^k and \dots and x_n is A_n^k , then y is W^k , $k = 1, \dots, l$, where $\mathbb{R}^{(k)}$ denotes the k -th rule, $1 \leq k \leq l$, $(x_1, x_2, \dots, x_n)^T \in \mathbb{U} \subset \mathbb{R}^n$, and $y \in \mathbb{R}$ are the linguistic variables that are associated with the inputs and output of the fuzzy logic system, respectively, and A_i^k and W^k denote the fuzzy sets in \mathbb{U} and \mathbb{R} . The fuzzy logic system performs a nonlinear mapping from \mathbb{U} to \mathbb{R} . In this paper, the fuzzy logic system is

$$y(x) = \frac{\sum_{k=1}^l y_k (\prod_{i=1}^n \mu_{A_i^k}(x_i))}{\sum_{k=1}^l (\prod_{i=1}^n \mu_{A_i^k}(x_i))} \quad (14)$$

where $x = [x_1, x_2, \dots, x_n]^T$ and $\mu_{A_i^k}(x_i)$ is the membership function of linguistic variable x_i with $\mu_{A_i^k}(x_i) = \exp[-\frac{(x_i - c_{ik}^2)}{\sigma_{ik}^2}]$. For clarify, the weight vector and fuzzy basis function vector are defined, respectively, as $\theta = [y_1, y_2, \dots, y_l]^T$ and $\phi(x, c, \sigma) = [s_1, s_2, \dots, s_l]^T$, where $s_k = \frac{\prod_{i=1}^n \mu_{A_i^k}(x_i)}{[\sum_{k=1}^l \prod_{i=1}^n \mu_{A_i^k}(x_i)]}$, $c = [c_1^T, c_2^T, \dots, c_n^T]^T$ and $\sigma = [\sigma_1^T, \sigma_2^T, \dots, \sigma_n^T]^T$. Therefore, (14) can be represented as

$$y = \theta^T \phi(x, c, \sigma) \quad (15)$$

It has been proven that the fuzzy logic system (15) has the capacity to approximate any given real continuous functions over a compact set to any degree of accuracy. Therefore, we have the following approximation for the unknown nonlinear function $f_i(x_i)$, $i = 1, 2, \dots, n$.

$$f_i(x_i) = \theta_i^{*T} \phi(x_i) + \epsilon_i \quad (16)$$

where θ_i^{*T} is an unknown constant parameter vector, $\phi(x_i)$ is the fuzzy basis function and ϵ_i is the approximation error, which satisfies $\max_{z \in \Omega_Z} \|\epsilon_i\| < \epsilon_i^*$, where $\epsilon_i^* > 0$ is unknown bound [63].

C. Preliminaries

To guarantee the time-varying constraint, we introduce the integral barrier Lyapunov function [64] as

$$V = \sum_{i=1}^n \int_0^{z_i} \frac{\sigma k_{ci}^2}{k_{ci}^2 - (\sigma + \alpha_i)^2} d\sigma \quad (17)$$

where $i = 1, \dots, n$, $z_i = x_i - \alpha_i$, and α_i is a continuously differentiable function satisfying $|\alpha_i| < k_{ci}$, $i = 1, \dots, n$. It is known that V is a continuously positive differentiable function over the set $\{|x_i| < k_{ci}\}$.

Lemma 1: (17) is a continuously positive differentiable function over the set $\{|x_i| < k_{ci}\}$. As for $|x_i| < k_{ci}$, $i = 1, \dots, n$, there is

$$\frac{z_i^2}{2} \leq V \leq \frac{k_{ci}^2 z_i^2}{k_{ci}^2 - x_i^2} \quad (18)$$

Proof: See the Appendix.

Remark 1: In (17), k_{ci} is a time-varying function and denotes the constrained upper bound of x_i , namely $\sup |x_i| < k_{ci}$, for $\forall t > 0$, given that initial value $|x_i(0)| < k_{ci}(0)$.

III. CONTROL DESIGN

For the robotic dynamics (10), it is tough to design a control policy to cope with the effect of time-varying constraints in the

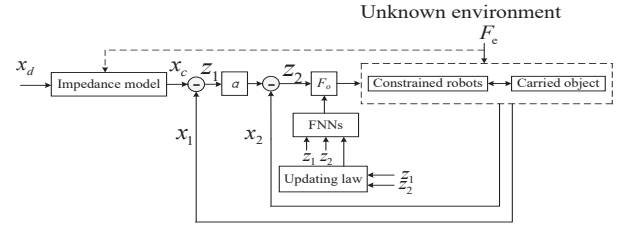


Fig. 2. System structure

presence of unknown environment. The problem is especially complex to solve full-state time-varying constraints. In this paper, the control schemes are proposed for the full-state time-varying constraint and the output time-varying constraint, respectively. Fig. 2 shows the system structure. To facilitate the control design, we define $x_1 = x_o$, $x_2 = \dot{x}_o$. The kinetic equation (10) can be rewritten as

$$\begin{aligned} \dot{x}_1 &= x_2 \\ \dot{x}_2 &= M^{-1}(F_o - F_e - G - Cx_2) \end{aligned} \quad (19)$$

where $x_1 = [x_{11}, \dots, x_{1n}]^T$, $x_2 = [x_{21}, \dots, x_{2n}]^T$. The error variables are defined as follows

$$\begin{aligned} z_1 &= x_1 - x_c \\ z_2 &= x_2 - \alpha \end{aligned} \quad (20)$$

where $z_1 = [z_{11}, \dots, z_{1n}]^T$, $z_2 = [z_{21}, \dots, z_{2n}]^T$, $x_c = [x_{c1}, \dots, x_{cn}]^T$, $\alpha = [\alpha_1, \dots, \alpha_n]^T$ is a virtual control aiming to make tracking error z_1 converge to a small region near zero.

A. Control Design with Output Constraint

In this section, system output x_1 should be demanded to be constrained by time-varying function $k_{ci} \in \mathbb{R}^+$, namely $|x_{1i}| < k_{ci}$, $i = 1, \dots, n$. To ensure this constraint, an integral barrier Lyapunov function is constructed as

$$V_1 = \sum_{i=1}^n \int_0^{z_{1i}} \frac{\sigma k_{ci}^2}{k_{ci}^2 - (\sigma + x_{ci})^2} d\sigma \quad (21)$$

The derivative of (21), with regard to time, is

$$\begin{aligned} \dot{V}_1 &= \sum_{i=1}^n \frac{\partial V_1}{\partial z_{1i}} \frac{dz_{1i}}{dt} + \sum_{i=1}^n \frac{\partial V_1}{\partial x_{ci}} \frac{dx_{ci}}{dt} + \sum_{i=1}^n \frac{\partial V_1}{\partial k_{ci}} \frac{dk_{ci}}{dt} \\ &= \sum_{i=1}^n \frac{k_{ci}^2 z_{1i}}{k_{ci}^2 - x_{1i}^2} (z_{2i} + \alpha_i - \dot{x}_{ci}) \\ &\quad + \sum_{i=1}^n z_{1i} \left(\frac{k_{ci}^2}{k_{ci}^2 - x_{1i}^2} - \rho_i \right) \dot{x}_{ci} + \sum_{i=1}^n \frac{\partial V_1}{\partial k_{ci}} \frac{dk_{ci}}{dt} \end{aligned} \quad (22)$$

where

$$\rho_{oi} = \frac{k_{ci}}{2z_{1i}} \ln \frac{(k_{ci} + z_{1i} + x_{ci})(k_{ci} - x_{ci})}{(k_{ci} - z_{1i} - x_{ci})(k_{ci} + x_{ci})} \quad (23)$$

Then, virtual control α_i , $i = 1, \dots, n$, is designed as

$$\alpha_i = -k_i z_{1i} + \frac{(k_{ci}^2 - x_{1i}^2) \dot{x}_{ci} \rho_i}{k_{ci}^2} - \frac{k_{ci}^2 - x_{1i}^2}{k_{ci}^2 z_{1i}} \frac{\partial V_1}{\partial k_{ci}} \frac{dk_{ci}}{dt} \quad (24)$$

where k_i , $i = 1, \dots, n$, is a positive constant.

Take virtual control α into (22), we further have

$$\dot{V}_1 = - \sum_{i=1}^n \frac{k_i k_{ci}^2 z_{1i}^2}{k_{ci}^2 - x_{1i}^2} + \sum_{i=1}^n \frac{k_{ci}^2 z_{1i} z_{2i}}{k_{ci}^2 - x_{1i}^2} \quad (25)$$

An integral barrier Lyapunov function is constructed as

$$V_2 = V_1 + \frac{1}{2} z_2^T M z_2 \quad (26)$$

Design the control input F_o^* as

$$F_o^* = - \begin{bmatrix} \frac{k_{c1}^2 z_{11}}{k_{c1}^2 - x_{11}^2} \\ \vdots \\ \frac{k_{cn}^2 z_{1n}}{k_{cn}^2 - x_{1n}^2} \end{bmatrix} - K_2 z_2 + F_e + G + C\alpha + M\dot{\alpha} \quad (27)$$

Substituting (24) and (27) into the time derivative of (26), we have

$$\begin{aligned} \dot{V}_2 &= - \sum_{i=1}^n \frac{k_i k_{ci}^2 z_{1i}^2}{k_{ci}^2 - x_{1i}^2} - z_2^T K_2 z_2 \\ &\leq - \sum_{i=1}^n \int_0^{z_{1i}} \frac{\sigma k_i k_{ci}^2}{k_{ci}^2 - (\sigma + x_{ci})^2} d\sigma - z_2^T K_2 z_2 \\ &\leq -\kappa_2 V_2 \end{aligned} \quad (28)$$

where $\kappa_2 = \min\{\min_{1 \leq i \leq n}(k_i), \frac{2\lambda_{\min}(K_2)}{\lambda_{\max}(M)}\}$. To ensure $\kappa_2 > 0$, parameters should satisfy $\min_{1 \leq i \leq n}(k_i) > 0, \frac{\lambda_{\min}(K_2)}{\lambda_{\max}(M)} > 0$. V_2 will converge into a small range near zero with the convergence rate $e^{-\kappa_2 t}$. But there are uncertainties in G, C, M , therefore F_o^* cannot be obtained in a real system. Fuzzy neural networks are used to approximate the uncertainties in G, C, M . An adaptive fuzzy neural network controller is designed as

$$F_o = - \begin{bmatrix} \frac{k_{c1}^2 z_{11}}{k_{c1}^2 - x_{11}^2} \\ \vdots \\ \frac{k_{cn}^2 z_{1n}}{k_{cn}^2 - x_{1n}^2} \end{bmatrix} - K_2 z_2 + F_e + \hat{\theta}_G^T \phi_G(Z_G) + \hat{\theta}_C^T \phi_C(Z_C)\alpha + \hat{\theta}_M^T \phi_M(Z_M)\dot{\alpha} + K_r \text{sgn}(z_2) \quad (29)$$

where $K_r = \text{diag}[k_{r1}, \dots, k_{rn}] > 0$; $\hat{\theta}_G, \hat{\theta}_C, \hat{\theta}_M$ are actual weight vectors, $\theta_G^*, \theta_C^*, \theta_M^*$ are optimal weight vectors, $\tilde{\theta}_G = \hat{\theta}_G - \theta_G^*, \tilde{\theta}_C = \hat{\theta}_C - \theta_C^*, \tilde{\theta}_M = \hat{\theta}_M - \theta_M^*$ are error weight vectors, $Z_G = [x_1^T, x_2^T]^T, Z_C = [x_1^T, x_2^T, \alpha^T]^T, Z_M = [x_1^T, x_2^T, \alpha^T, \dot{\alpha}^T]^T$ are fuzzy neural network inputs, respectively.

To improve the system control performance, we design the updating laws as

$$\dot{\hat{\theta}}_{Gi} = -\Gamma_{Gi}(\phi_{Gi}(Z_G)z_{2i} + \sigma_G \hat{\theta}_{Gi}) \quad (30)$$

$$\dot{\hat{\theta}}_{Ci} = -\Gamma_{Ci}(\phi_{Ci}(Z_C)z_{2i}\alpha_i + \sigma_C \hat{\theta}_{Ci}) \quad (31)$$

$$\dot{\hat{\theta}}_{Mi} = -\Gamma_{Mi}(\phi_{Mi}(Z_M)z_{2i}\dot{\alpha}_i + \sigma_M \hat{\theta}_{Mi}) \quad (32)$$

where $\Gamma_{Gi}, \Gamma_{Ci}, \Gamma_{Mi}$ are positive definite symmetric matrixes, $\sigma_G, \sigma_C, \sigma_M$ are positive constants, $\hat{\theta}_G^T \phi_G, \hat{\theta}_C^T \phi_C, \hat{\theta}_M^T \phi_M$ are

estimated values of $\theta_G^{*T} \phi_G, \theta_C^{*T} \phi_C, \theta_M^{*T} \phi_M$, respectively.

$$\theta_G^{*T} \phi_G = G + \epsilon_G \quad (33)$$

$$\theta_C^{*T} \phi_C = C + \epsilon_C \quad (34)$$

$$\theta_M^{*T} \phi_M = M + \epsilon_M \quad (35)$$

where $\epsilon_G, \epsilon_C, \epsilon_M$ are approximation errors satisfying $\|\epsilon_G\| \leq \bar{\epsilon}_G, \|\epsilon_C\| \leq \bar{\epsilon}_C, \|\epsilon_M\| \leq \bar{\epsilon}_M$, with $\bar{\epsilon}_G, \bar{\epsilon}_C, \bar{\epsilon}_M$ being positive constants.

Choose a positive Lyapunov function as

$$\begin{aligned} V_3 &= \sum_{i=1}^n \int_0^{z_{1i}} \frac{\sigma k_{ci}^2}{k_{ci}^2 - (\sigma + x_{di})^2} d\sigma + \frac{1}{2} z_2^T M z_2 \\ &\quad + \frac{1}{2} \sum_{i=1}^n \tilde{\theta}_{Gi}^T \Gamma_{Gi}^{-1} \tilde{\theta}_{Gi} + \frac{1}{2} \sum_{i=1}^n \tilde{\theta}_{Ci}^T \Gamma_{Ci}^{-1} \tilde{\theta}_{Ci} \\ &\quad + \frac{1}{2} \sum_{i=1}^n \tilde{\theta}_{Mi}^T \Gamma_{Mi}^{-1} \tilde{\theta}_{Mi} \end{aligned} \quad (36)$$

Substituting (24) and (29) into the time derivative of (36), we have

$$\begin{aligned} \dot{V}_3 &= - \sum_{i=1}^n \frac{k_i k_{ci}^2 z_{1i}^2}{k_{ci}^2 - x_{1i}^2} - z_2^T K_2 z_2 + z_2^T (\tilde{\theta}_G^T \phi_G(Z_G) \\ &\quad + \tilde{\theta}_C^T \phi_C(Z_C) + \tilde{\theta}_M^T \phi_M(Z_M) - \epsilon_G - \epsilon_C \alpha - \epsilon_M \dot{\alpha} \\ &\quad + K_r \text{sgn}(z_2)) + \sum_{i=1}^n \tilde{\theta}_{Gi}^T \Gamma_{Gi}^{-1} \dot{\tilde{\theta}}_{Gi} + \sum_{i=1}^n \tilde{\theta}_{Ci}^T \Gamma_{Ci}^{-1} \dot{\tilde{\theta}}_{Ci} \\ &\quad + \sum_{i=1}^n \tilde{\theta}_{Mi}^T \Gamma_{Mi}^{-1} \dot{\tilde{\theta}}_{Mi} \end{aligned} \quad (37)$$

Let us define $(\epsilon_G + \epsilon_C \alpha + \epsilon_M \dot{\alpha})_i$ as $E_i, i = 1, \dots, n$, for the interval $t \in [0, +\infty)$, where $(\cdot)_i$ is i -th element of a vector. Therefore, we obtain $E = [E_1, \dots, E_n]^T$.

Substituting the weight updating laws into (37), we have

$$\begin{aligned} \dot{V}_3 &= - \sum_{i=1}^n \frac{k_i k_{ci}^2 z_{1i}^2}{k_{ci}^2 - x_{1i}^2} - z_2^T K_2 z_2 + z_2^T (K_r \text{sgn}(z_2) - E) \\ &\quad + z_2^T (\tilde{\theta}_G^T \phi_G(Z_G) + \tilde{\theta}_C^T \phi_C(Z_C)\alpha + \tilde{\theta}_M^T \phi_M(Z_M)\dot{\alpha}) \\ &\quad - \sum_{i=1}^n \tilde{\theta}_{Gi}^T (\phi_{Gi}(Z_G)z_{2i} + \sigma_G \hat{\theta}_{Gi}) \\ &\quad - \sum_{i=1}^n \tilde{\theta}_{Ci}^T (\phi_{Ci}(Z_C)z_{2i}\alpha_i + \sigma_C \hat{\theta}_{Ci}) \\ &\quad - \sum_{i=1}^n \tilde{\theta}_{Mi}^T (\phi_{Mi}(Z_M)z_{2i}\dot{\alpha}_i + \sigma_M \hat{\theta}_{Mi}) \end{aligned} \quad (38)$$

Notice that

$$z_2^T \tilde{\theta}_G^T \phi_G(Z_G) = \sum_{i=1}^n \tilde{\theta}_{Gi}^T \phi_{Gi}(Z_G)z_{2i} \quad (39)$$

$$z_2^T \tilde{\theta}_C^T \phi_C(Z_C)\alpha = \sum_{i=1}^n \tilde{\theta}_{Ci}^T \phi_{Ci}(Z_C)z_{2i}\alpha_i \quad (40)$$

$$z_2^T \tilde{\theta}_M^T \phi_M(Z_M)\dot{\alpha} = \sum_{i=1}^n \tilde{\theta}_{Mi}^T \phi_{Mi}(Z_M)z_{2i}\dot{\alpha}_i \quad (41)$$

and the gain K_r is designed to satisfy $|E_i| \leq k_{ri}, i = 1, \dots, n$,

we have $z_2^T(K_r \text{sgn}(z_2) - E) \leq 0$, therefore

$$\begin{aligned} \dot{V}_3 \leq & - \sum_{i=1}^n \frac{k_i k_{ci}^2 z_{1i}^2}{k_{ci}^2 - x_{1i}^2} - z_2^T K_2 z_2 - \sum_{i=1}^n \tilde{\theta}_{Gi}^T \sigma_G \hat{\theta}_{Gi} \\ & - \sum_{i=1}^n \tilde{\theta}_{Ci}^T \sigma_C \hat{\theta}_{Ci} - \sum_{i=1}^n \tilde{\theta}_{Mi}^T \sigma_M \hat{\theta}_{Mi} \end{aligned} \quad (42)$$

Since $-\sum_{i=1}^n \tilde{\theta}_{Gi}^T \sigma_{Gi} \hat{\theta}_{Gi} \leq -\frac{\sigma_{Gi}}{2} \sum_{i=1}^n \tilde{\theta}_{Gi}^T \tilde{\theta}_{Gi} + \frac{\sigma_{Gi}}{2} \sum_{i=1}^n \theta_{Gi}^* \theta_{Gi}^*$, $-\sum_{i=1}^n \tilde{\theta}_{Ci}^T \sigma_{Ci} \hat{\theta}_{Ci} \leq -\frac{\sigma_{Ci}}{2} \sum_{i=1}^n \tilde{\theta}_{Ci}^T \tilde{\theta}_{Ci} + \frac{\sigma_{Ci}}{2} \sum_{i=1}^n \theta_{Ci}^* \theta_{Ci}^*$ and $-\sum_{i=1}^n \tilde{\theta}_{Mi}^T \sigma_{Mi} \hat{\theta}_{Mi} \leq -\frac{\sigma_{Mi}}{2} \sum_{i=1}^n \tilde{\theta}_{Mi}^T \tilde{\theta}_{Mi} + \frac{\sigma_{Mi}}{2} \sum_{i=1}^n \theta_{Mi}^* \theta_{Mi}^*$, we have

$$\begin{aligned} \dot{V}_3 \leq & - \sum_{i=1}^n \frac{k_i k_{ci}^2 z_{1i}^2}{k_{ci}^2 - x_{1i}^2} - \frac{\sigma_{Gi}}{2} \sum_{i=1}^n \tilde{\theta}_{Gi}^T \tilde{\theta}_{Gi} - \frac{\sigma_{Ci}}{2} \sum_{i=1}^n \tilde{\theta}_{Ci}^T \tilde{\theta}_{Ci} \\ & - \frac{\sigma_{Mi}}{2} \sum_{i=1}^n \tilde{\theta}_{Mi}^T \tilde{\theta}_{Mi} + \frac{\sigma_{Gi}}{2} \sum_{i=1}^n \theta_{Gi}^* \theta_{Gi}^* - z_2^T K_2 z_2 \\ & + \frac{\sigma_{Ci}}{2} \sum_{i=1}^n \theta_{Ci}^* \theta_{Ci}^* + \frac{\sigma_{Mi}}{2} \sum_{i=1}^n \theta_{Mi}^* \theta_{Mi}^* \\ \leq & -\kappa_3 V_3 + C_3 \end{aligned} \quad (43)$$

where

$$\begin{aligned} \kappa_3 = & \min\{k_1, \dots, k_n, \frac{2\lambda_{\min}(K_2)}{\lambda_{\max}(M)}, \frac{\sigma_{Gi}}{\lambda_{\max}(\Gamma_{Gi}^{-1})}, \frac{\sigma_{Ci}}{\lambda_{\max}(\Gamma_{Ci}^{-1})}, \\ & \frac{\sigma_{Mi}}{\lambda_{\max}(\Gamma_{Mi}^{-1})}\} \\ C_3 = & \frac{\sigma_{Gi}}{2} \sum_{i=1}^n \theta_{Gi}^* \theta_{Gi}^* + \frac{\sigma_{Ci}}{2} \sum_{i=1}^n \theta_{Ci}^* \theta_{Ci}^* + \frac{\sigma_{Mi}}{2} \sum_{i=1}^n \theta_{Mi}^* \theta_{Mi}^* \end{aligned}$$

To ensure $\kappa_3 > 0$, $C_3 > 0$, controller parameters should satisfy $k_i > 0$, $\lambda_{\max}(K_2) > 0$, $\sigma_{Gi} > 0$, $\sigma_{Ci} > 0$ and $\sigma_{Mi} > 0$, $i = 1, \dots, n$. Therefore, we know that V_3 is bounded for $\forall t > 0$.

Theorem 1: For the robot system (10) with output time-varying constraint, and FNN control (29) with updating law (31)-(33) and impedance learning (13), given that initial conditions are bounded. It can be concluded that target impedance is achieved and the tracking errors are uniformly bounded ultimately. The tracking errors converge to a small range near zero and the range can be changed by choosing appropriate parameters. The system output is constrained by the predefined constraint region the user defines. The tracking error z_1 converges to the compact set $\Omega_{z_1} := \{z_1 \in \mathbb{R}^n \mid \|z_{1i}\| \leq \sqrt{2B}, i = 1, \dots, n\}$. The tracking error z_2 converges to the compact set $\Omega_{z_2} := \{z_2 \in \mathbb{R}^n \mid \|z_{2i}\| \leq \sqrt{2B}, i = 1, \dots, n\}$, where $B := V_3(0) + \frac{C_3}{\kappa_3}$.

Proof: See the Appendix.

B. Control Design with Full-State Constraint

The FNN control with the full-state constraint will be presented in this section. It should be emphasized that although the control design is similar to the control (29), the system states should be demanded to be constrained by the time-varying constraint in the control design. In this sense, the system state x_2 should be constrained satisfying $|x_{2i}| \leq k_{di}$ for $\forall t > 0$ where $k_{di} \in \mathbb{R}^+$, $i = 1, \dots, n$, is a time-varying function. The detailed design is presented as follows. To ensure that system states remain in the predefined constraint region,

a positive integral barrier Lyapunov function is constructed as

$$V_5 = V_2 + V_4 \quad (44)$$

where

$$V_4 = \sum_{i=1}^n \int_0^{z_{2i}} \frac{\sigma k_{di}^2}{k_{di}^2 - (\sigma + \alpha_i)^2} d\sigma \quad (45)$$

The derivative of V_5 , with respect to time, is

$$\begin{aligned} \dot{V}_5 = & \dot{V}_2 + \sum_{i=1}^n \frac{\partial V_4}{\partial z_{2i}} \frac{dz_{2i}}{dt} + \sum_{i=1}^n \frac{\partial V_4}{\partial \alpha_i} \frac{d\alpha_i}{dt} + \sum_{i=1}^n \frac{\partial V_4}{\partial k_{di}} \frac{dk_{di}}{dt} \\ = & \dot{V}_2 + \sum_{i=1}^n \frac{k_{di}^2 z_{2i} \dot{z}_{2i}}{k_{di}^2 - x_{2i}^2} + \sum_{i=1}^n z_{2i} \left(\frac{k_{di}^2}{k_{di}^2 - x_{2i}^2} - \rho_{2i} \right) \dot{\alpha}_i \\ & + \sum_{i=1}^n \frac{\partial V_4}{\partial k_{di}} \frac{dk_{di}}{dt} \end{aligned} \quad (46)$$

where

$$\rho_{2i} = \frac{k_{di}}{2z_{2i}} \ln \frac{(k_{di} + z_{2i} + \alpha_i)(k_{di} - \alpha_i)}{(k_{di} - z_{2i} - \alpha_i)(k_{di} + \alpha_i)} \quad (47)$$

The model-based controller is designed as

$$\begin{aligned} F_o^* = & - \begin{bmatrix} \frac{k_{c1}^2 z_{11}}{k_{c1}^2 - x_{11}^2} \\ \vdots \\ \frac{k_{cn}^2 z_{1n}^2}{k_{cn}^2 - x_{1n}^2} \end{bmatrix} - \begin{bmatrix} \frac{k_{d1}^2 k_{11} z_{21}}{k_{d1}^2 - x_{21}^2} \\ \vdots \\ \frac{k_{dn}^2 k_{1n} z_{2n}}{k_{dn}^2 - x_{2n}^2} \end{bmatrix} \\ & - \begin{bmatrix} \left(\frac{k_{d1}^2}{k_{d1}^2 - x_{21}^2} - \rho_{21} \right) \dot{\alpha}_1 \\ \vdots \\ \left(\frac{k_{dn}^2}{k_{dn}^2 - x_{2n}^2} - \rho_{2n} \right) \dot{\alpha}_n \end{bmatrix} - \sum_{i=1}^n \frac{1}{z_{2i}} \frac{\partial V_4}{\partial k_{di}} \frac{dk_{di}}{dt} \\ & - K_2 z_2 + F_e + G + C\alpha + M\dot{\alpha} \end{aligned} \quad (48)$$

where $k_{1i}, i = 1, \dots, n$, is a positive constant.

Substituting (24) and (48) into (46), we have

$$\begin{aligned} \dot{V}_5 = & - \sum_{i=1}^n \frac{k_i k_{ci}^2 z_{1i}^2}{k_{ci}^2 - x_{1i}^2} - \sum_{i=1}^n \frac{k_{1i} k_{di}^2 z_{2i}^2}{k_{di}^2 - x_{2i}^2} + \sum_{i=1}^n \frac{k_{di}^2 z_{2i} \dot{z}_{2i}}{k_{di}^2 - x_{2i}^2} \\ & - z_2^T K_2 z_2 \leq -\kappa_5 V_5 + \sum_{i=1}^n \frac{k_{di}^2 z_{2i} \dot{z}_{2i}}{k_{di}^2 - x_{2i}^2} \end{aligned} \quad (49)$$

where

$$\kappa_5 = \min\left\{ \min_{1 \leq i \leq n} k_i, \min_{1 \leq i \leq n} k_{1i}, \frac{2\lambda_{\min}(K_2)}{\lambda_{\max}(M)} \right\} \quad (50)$$

Multiplying (49) by $e^{\kappa_5 t}$ yields

$$e^{\kappa_5 t} \dot{V}_5 \leq -\kappa_5 e^{\kappa_5 t} V_5 + e^{\kappa_5 t} g(t) N(z_2) \dot{z}_2 \quad (51)$$

where $g(t) = \text{diag}\left[\frac{k_{d1}^2}{(k_{d1}^2 - x_{21}^2) \cos(\frac{\pi}{2} z_{21})}, \dots, \frac{k_{dn}^2}{(k_{dn}^2 - x_{2n}^2) \cos(\frac{\pi}{2} z_{2n})}\right]$, $N(z_2) = [z_{21} \cos(\frac{\pi}{2} z_{21}), \dots, z_{2n} \cos(\frac{\pi}{2} z_{2n})]^T$. Integrating (51), yields

$$V_5(t) \leq e^{-\kappa_5 t} V_5(0) + e^{-\kappa_5 t} \int_0^t g(\tau) N(z_2) \dot{z}_2 e^{\tau t} d\tau \quad (52)$$

where $t \in [0, t_f)$. According to [36], we know that $\|\int_0^t g(\tau) N(z_2) \dot{z}_2 e^{\tau t} d\tau\|$ is bounded. Therefore, define \mathcal{N} as an upper bound of $\|\int_0^t g(\tau) N(z_2) \dot{z}_2 e^{\tau t} d\tau\|$, namely $\|\int_0^t g(\tau) N(z_2) \dot{z}_2 e^{\tau t} d\tau\| \leq \mathcal{N}$. Therefore, it can be concluded

ed that $V_5(t), z_1, z_2$ are bounded on $[0, t_f]$ if $\kappa_5 > 0$. However, the uncertainties exist in M, C, G, F_o^* is not available in a real system. FNNs have the ability to approximate nonlinear functions in ideal accuracy, thus in this section FNNs are used to approximate M, C, G , respectively. An adaptive FNN controller is designed as

$$F_o = - \begin{bmatrix} \frac{k_{c1}^2 z_{11}}{k_{c1}^2 - x_{11}^2} \\ \vdots \\ \frac{k_{cn}^2 z_{1n}}{k_{cn}^2 - x_{1n}^2} \end{bmatrix} - \begin{bmatrix} \frac{k_{d1}^2 k_{11} z_{21}}{k_{d1}^2 - x_{21}^2} \\ \vdots \\ \frac{k_{dn}^2 k_{1n} z_{2n}}{k_{dn}^2 - x_{2n}^2} \end{bmatrix} - \begin{bmatrix} (\frac{k_{d1}^2}{k_{d1}^2 - x_{21}^2} - \rho_{21}) \dot{\alpha}_1 \\ \vdots \\ (\frac{k_{dn}^2}{k_{dn}^2 - x_{2n}^2} - \rho_{2n}) \dot{\alpha}_n \end{bmatrix} - \sum_{i=1}^n \frac{1}{z_{2i}} \frac{\partial V_4}{\partial k_{di}} \frac{dk_{di}}{dt} - K_2 z_2 + F_e + \tilde{\theta}_G^T \phi_G(Z_G) + \tilde{\theta}_C^T \phi_C(Z_C) \alpha + \tilde{\theta}_M^T \phi_M(Z_M) \dot{\alpha} + K_r \text{sgn}(z_2) \quad (53)$$

A Lyapunov function is constructed as

$$V_6 = V_5 + \frac{1}{2} \sum_{i=1}^n \tilde{\theta}_{Gi}^T \Gamma_{Gi}^{-1} \tilde{\theta}_{Gi} + \frac{1}{2} \sum_{i=1}^n \tilde{\theta}_{Ci}^T \Gamma_{Ci}^{-1} \tilde{\theta}_{Ci} + \frac{1}{2} \sum_{i=1}^n \tilde{\theta}_{Mi}^T \Gamma_{Mi}^{-1} \tilde{\theta}_{Mi} \quad (54)$$

Substituting (24) and (53) into the time derivative of V_6 , we have

$$\dot{V}_6 = - \sum_{i=1}^n \frac{k_i k_{ci}^2 z_{1i}^2}{k_{ci}^2 - x_{1i}^2} - \sum_{i=1}^n \frac{k_{1i} k_{di}^2 z_{2i}^2}{k_{di}^2 - x_{2i}^2} + \sum_{i=1}^n \frac{k_{di}^2 z_{2i} \dot{z}_{2i}}{k_{di}^2 - x_{2i}^2} - z_2^T K_2 z_2 + z_2^T (\tilde{\theta}_G^T \phi_G(Z_G) + \tilde{\theta}_C^T \phi_C(Z_C) + \tilde{\theta}_M^T \phi_M(Z_M) - \epsilon_G - \epsilon_C \alpha - \epsilon_M \dot{\alpha} + K_r \text{sgn}(z_2)) + \sum_{i=1}^n \tilde{\theta}_{Gi}^T \Gamma_{Gi}^{-1} \dot{\tilde{\theta}}_{Gi} + \sum_{i=1}^n \tilde{\theta}_{Ci}^T \Gamma_{Ci}^{-1} \dot{\tilde{\theta}}_{Ci} + \sum_{i=1}^n \tilde{\theta}_{Mi}^T \Gamma_{Mi}^{-1} \dot{\tilde{\theta}}_{Mi} \quad (55)$$

Let us define $(\epsilon_G + \epsilon_C \alpha + \epsilon_M \dot{\alpha})_i$ as $E_i, i = 1, \dots, n$, for the interval $t \in [0, +\infty)$, where $(\cdot)_i$ is i th element of a vector. Therefore, we obtain $E = [E_1, \dots, E_n]^T$. Substituting (31)-(33) and (40)-(42) into (55), we have

$$\dot{V}_6 \leq - \sum_{i=1}^n \frac{k_i k_{ci}^2 z_{1i}^2}{k_{ci}^2 - x_{1i}^2} - \sum_{i=1}^n \frac{k_{1i} k_{di}^2 z_{2i}^2}{k_{di}^2 - x_{2i}^2} + \sum_{i=1}^n \frac{k_{di}^2 z_{2i} \dot{z}_{2i}}{k_{di}^2 - x_{2i}^2} - z_2^T K_2 z_2 + z_2^T (K_r \text{sgn}(z_2) - E) - \sum_{i=1}^n \tilde{\theta}_{Gi}^T \sigma_G \hat{\theta}_{Gi} - \sum_{i=1}^n \tilde{\theta}_{Ci}^T \sigma_C \hat{\theta}_{Ci} - \sum_{i=1}^n \tilde{\theta}_{Mi}^T \sigma_M \hat{\theta}_{Mi} \quad (56)$$

The gain K_r is designed to satisfy $|E_i| \leq k_{ri}, i = 1, \dots, n$,

we have $z_2^T (K_r \text{sgn}(z_2) - E) \leq 0$. And since

$$- \sum_{i=1}^n \tilde{\theta}_{Gi}^T \sigma_{Gi} \hat{\theta}_{Gi} \leq - \frac{\sigma_{Gi}}{2} \sum_{i=1}^n \tilde{\theta}_{Gi}^T \tilde{\theta}_{Gi} + \frac{\sigma_{Gi}}{2} \sum_{i=1}^n \theta_{Gi}^{*T} \theta_{Gi}^* - \sum_{i=1}^n \tilde{\theta}_{Ci}^T \sigma_{Ci} \hat{\theta}_{Ci} \leq - \frac{\sigma_{Ci}}{2} \sum_{i=1}^n \tilde{\theta}_{Ci}^T \tilde{\theta}_{Ci} + \frac{\sigma_{Ci}}{2} \sum_{i=1}^n \theta_{Ci}^{*T} \theta_{Ci}^* - \sum_{i=1}^n \tilde{\theta}_{Mi}^T \sigma_{Mi} \hat{\theta}_{Mi} \leq - \frac{\sigma_{Mi}}{2} \sum_{i=1}^n \tilde{\theta}_{Mi}^T \tilde{\theta}_{Mi} + \frac{\sigma_{Mi}}{2} \sum_{i=1}^n \theta_{Mi}^{*T} \theta_{Mi}^*$$

we have

$$\dot{V}_6 \leq - \sum_{i=1}^n \frac{k_i k_{ci}^2 z_{1i}^2}{k_{ci}^2 - x_{1i}^2} - \sum_{i=1}^n \frac{k_{1i} k_{di}^2 z_{2i}^2}{k_{di}^2 - x_{2i}^2} + \sum_{i=1}^n \frac{k_{di}^2 z_{2i} \dot{z}_{2i}}{k_{di}^2 - x_{2i}^2} - z_2^T K_2 z_2 - \frac{\sigma_{Gi}}{2} \sum_{i=1}^n \tilde{\theta}_{Gi}^T \tilde{\theta}_{Gi} - \frac{\sigma_{Ci}}{2} \sum_{i=1}^n \tilde{\theta}_{Ci}^T \tilde{\theta}_{Ci} - \frac{\sigma_{Mi}}{2} \sum_{i=1}^n \tilde{\theta}_{Mi}^T \tilde{\theta}_{Mi} + \frac{\sigma_{Gi}}{2} \sum_{i=1}^n \theta_{Gi}^{*T} \theta_{Gi}^* + \frac{\sigma_{Ci}}{2} \sum_{i=1}^n \theta_{Ci}^{*T} \theta_{Ci}^* + \frac{\sigma_{Mi}}{2} \sum_{i=1}^n \theta_{Mi}^{*T} \theta_{Mi}^* \leq -\kappa_6 V_6 + C_6 + \sum_{i=1}^n \frac{k_{di}^2 z_{2i} \dot{z}_{2i}}{k_{di}^2 - x_{2i}^2} \quad (57)$$

where

$$\kappa_6 = \min \left\{ \min_{1 \leq i \leq n} (k_i), \min_{1 \leq i \leq n} (k_{1i}), \frac{2\lambda_{\min}(K_2)}{\lambda_{\max}(M)}, \frac{\sigma_{Gi}}{\lambda_{\max}(\Gamma_{Gi})}, \frac{\sigma_{Ci}}{\lambda_{\max}(\Gamma_{Ci})}, \frac{\sigma_{Mi}}{\lambda_{\max}(\Gamma_{Mi})} \right\} C_6 = \frac{\sigma_{Gi}}{2} \sum_{i=1}^n \theta_{Gi}^{*T} \theta_{Gi}^* + \frac{\sigma_{Ci}}{2} \sum_{i=1}^n \theta_{Ci}^{*T} \theta_{Ci}^* + \frac{\sigma_{Mi}}{2} \sum_{i=1}^n \theta_{Mi}^{*T} \theta_{Mi}^*$$

Multiplying (57) by $e^{\kappa_6 t}$ yields

$$e^{\kappa_6 t} \dot{V}_6 \leq -\kappa_6 e^{\kappa_6 t} V_6 + e^{\kappa_6 t} \frac{C_6}{\kappa_6} + e^{\kappa_6 t} g(t) N(z_2) \dot{z}_2 \quad (58)$$

where $g(t) = \text{diag}[\frac{k_{d1}^2}{(k_{d1}^2 - x_{21}^2) \cos(\frac{\pi}{2} z_{21})}, \dots, \frac{k_{dn}^2}{(k_{dn}^2 - x_{2n}^2) \cos(\frac{\pi}{2} z_{2n})}]$, $N(z_2) = [z_{21} \cos(\frac{\pi}{2} z_{21}), \dots, z_{2n} \cos(\frac{\pi}{2} z_{2n})]^T$. Integrating (58), yields

$$V_6(t) \leq e^{-\kappa_6 t} V_6(0) + \frac{C_6}{\kappa_6} + e^{-\kappa_6 t} \int_0^t g(\tau) N(z_2) \dot{z}_2 e^{\tau t} d\tau \quad (59)$$

where $t \in [0, t_f]$. According to [36], we know that $\|\int_0^t g(\tau) N(z_2) \dot{z}_2 e^{\tau t} d\tau\|$ is bounded. Therefore, define \mathcal{N} as an upper bound of $\|\int_0^t g(\tau) N(z_2) \dot{z}_2 e^{\tau t} d\tau\|$, namely $\|\int_0^t g(\tau) N(z_2) \dot{z}_2 e^{\tau t} d\tau\| \leq \mathcal{N}$. To ensure that $\kappa_6 > 0, C_6 > 0$, controller parameters should satisfy $\min_{1 \leq i \leq n} (k_i) > 0, \min_{1 \leq i \leq n} (k_{1i}) > 0, \frac{2\lambda_{\min}(K_2)}{\lambda_{\max}(M)} > 0, \frac{\sigma_{Gi}}{\lambda_{\max}(\Gamma_{Gi})} > 0, \frac{\sigma_{Ci}}{\lambda_{\max}(\Gamma_{Ci})} > 0, \frac{\sigma_{Mi}}{\lambda_{\max}(\Gamma_{Mi})} > 0$. Therefore, V_6 is bounded.

Theorem 2: For the robotic system (10) with full-state time-varying constraints, and FNN control (53) with updating law (31)-(33) and impedance learning (13), given that initial conditions are bounded. It can be concluded that target impedance is achieved and the tracking errors are uniformly bounded ultimately. The tracking errors converge to a small

range near zero and the range can be changed by choosing appropriate parameters. The system states are constrained by the predefined constraint region the user defines. The tracking error z_1 converges to the compact set $\Omega_{z_1} := \{z_1 \in \mathbb{R}^n \mid |z_{1i}| \leq \sqrt{2B_1}, i = 1, \dots, n\}$. The tracking error z_2 converges to the compact set $\Omega_{z_2} := \{z_2 \in \mathbb{R}^n \mid |z_{2i}| \leq \sqrt{2B_1}, i = 1, \dots, n\}$, where $B_1 := V_6(0) + \frac{C_6}{\kappa_6} + \mathcal{N}$.

Proof: See the Appendix.

IV. SIMULATION

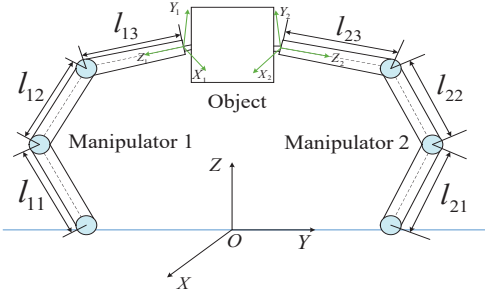


Fig. 3. Simulation scenario.

In this section, an environment-robot interaction system is considered to verify the effectiveness of the proposed control (29) and (53), respectively. The environment-robot interaction system includes two robots sharing the same system parameters and 3 degrees of freedom including three rotary degrees, an object and a force sensor located on the surface of the object as shown in Fig. 3. In Fig. 3, let m_{i1} , m_{i2} and m_{i3} denote the mass of link 1, link 2 and link 3 of manipulator i , $i = 1, 2$, respectively, let l_{i1} , l_{i2} and l_{i3} denote the length of link 1, link 2 and link 3 of manipulator i , $i = 1, 2$, respectively, and let I_{ji} denote the moment of inertia of link j , $j = 1, 2, 3$, of manipulator i , $i = 1, 2$, with regard to an axis coming out of the page passing through the center of mass of link i . Simulation time is $t_f = 20$ s. The sampling period is 0.0025s.

The trajectory commanded by the user is given by

$$x_d = \begin{bmatrix} x_{d1} \\ x_{d2} \\ x_{d3} \end{bmatrix} = \begin{bmatrix} 0.8 \\ 0.8 + 0.2 \sin(t) \\ 0.8 - 0.2 \cos(t) \end{bmatrix} \text{ m} \quad (60)$$

which is a circle with center of a circle at $[0.8, 0.8, 0.8]^T$ m and radius being 0.2m. The robot is initially at rest with $x_1(0) = [0.201, 0.801, 0.601]^T$ m, $\dot{x}_1(0) = [0, 0, 0]^T$ m/s.

The system parameters (see [8]) of the object is given by

$$M_o = \begin{bmatrix} m_o & 0 & 0 \\ 0 & m_o & 0 \\ 0 & 0 & 1 \end{bmatrix}, G_o = \begin{bmatrix} 0 \\ 0 \\ -m_o g \end{bmatrix} \quad (61)$$

where m_o denotes object weight, g denotes gravitational acceleration. Adjacency matrix J_o (see [8]) is given by

$$J_o = \begin{bmatrix} 1 & 0 & 0 \\ 0 & 1 & 0 \\ l_{13} \sin(x_{12}) & -l_{13} \cos(x_{12}) & 1 \\ 1 & 0 & 0 \\ 0 & 1 & 0 \\ -l_{23} \sin(x_{13}) & l_{23} \cos(x_{13}) & 1 \end{bmatrix} \quad (62)$$

The system parameters of i -th ($i = 1, 2$) robotic manipulator are given by

$$D_i = \begin{bmatrix} D_{i11} & D_{i12} & D_{i13} \\ D_{i21} & D_{i22} & D_{i23} \\ D_{i31} & D_{i32} & D_{i33} \end{bmatrix} \quad (63)$$

$$C_i = \begin{bmatrix} C_{i11} & C_{i12} & C_{i13} \\ C_{i21} & C_{i22} & C_{i23} \\ C_{i31} & C_{i32} & C_{i33} \end{bmatrix}, G_i = \begin{bmatrix} G_{i1} \\ G_{i2} \\ G_{i3} \end{bmatrix} \quad (64)$$

where $D_{i11} = m_{i3}q_{i3}^2 \sin^2(q_{i2}) + p_{i1}$; $D_{i12} = p_{i2}q_{i3} \cos(q_{i2})$; $D_{i13} = p_{i2} \sin(q_{i2})$; $D_{i21} = p_{i2}q_{i3} \cos(q_{i2})$; $D_{i22} = m_{i3}q_{i3}^2 + I_{i2}$; $D_{i23} = 0$; $D_{i31} = p_{i2} \sin(q_{i2})$; $D_{i32} = 0$; $D_{i33} = m_{i3}$; $C_{i11} = p_{i4}\dot{q}_{i2} + p_{i5}\dot{q}_{i3}$; $C_{i12} = p_{i4}\dot{q}_{i1} - p_{i3}q_{i3}p_{i8}$; $C_{i13} = p_{i5}\dot{q}_{i1} - p_{i3}p_{i6}q_{i3}$; $C_{i21} = -p_{i4}\dot{q}_{i1}$; $C_{i22} = m_{i3}q_{i3}\dot{q}_{i3}$; $C_{i23} = p_{i3}p_{i9} - m_{i3}q_{i3}\dot{q}_{i2}$; $C_{i31} = -p_{i5}\dot{q}_{i1} + p_{i3}p_{i10}$; $C_{i32} = m_{i3}q_{i3}\dot{q}_{i2} + p_{i3}p_{i11}$; $C_{i33} = 0$; $G_{i1} = 0$; $G_{i2} = -m_{i3}gq_{i3} \cos(q_{i2})$; $G_{i3} = -m_{i3}g \sin(q_{i2})$. where $p_{i1} = m_{i3}l_{i2}^2 + m_{i2}l_{i1}^2 + I_{i1}$; $p_{i2} = m_{i3}l_{i2}$; $p_{i3} = m_{i3}l_{i1}$; $p_{i4} = m_{i3}q_{i3}^2 \sin(q_{i2}) \cos(q_{i2})$; $p_{i5} = m_{i3}q_{i3}^2 \sin^2(q_{i2})$; $p_{i6} = \sin(q_{i2})\dot{q}_{i2}$; $p_{i7} = \sin(q_{i2})\dot{q}_{i3}$; $p_{i8} = p_{i6} + p_{i7}$; $p_{i9} = \cos(q_{i2})\dot{q}_{i1}$; $p_{i10} = \cos(q_{i2})\dot{q}_{i2}$ and $p_{i11} = \cos(q_{i2})\dot{q}_{i3}$. Parameters of the robotic system are defined in the table below.

Table 1: Parameters of the robot

Parameter	Description	Value
m_{i1}	Mass of link 1	2.00 kg
m_{i2}	Mass of link 2	1.00 kg
m_{i3}	Mass of link 3	0.30 kg
l_{i1}	Length of link 1	1.00 m
l_{i2}	Length of link 2	0.20 m
l_{i3}	Length of link 3	1.00 m
I_{i1}	Inertia of link 1	$0.5 \times 10^{-3} \text{ kgm}^2$
I_{i2}	Inertia of link 2	$0.1 \times 10^{-3} \text{ kgm}^2$

To further verify the performance of the proposed control in different environments, four cases are implemented, respectively. Case one and Case three denote that the object carried two robots move in a free space without force from the environment. Case two and Case four denote that the object carried two robots move with force from the environment. The detailed simulation procedure is specified later. In the subsequent expression, without force from the environment denotes $F_e = 0$, and with force from the environment denotes $F_e \neq 0$. If $F_e = 0$, it is known that $x_c = x_d$ according to impedance model (13).

A. Control Design with Output Constraint

Case one: In the first case, the simulation procedure is that carried by two robots, the object moves along a circular trajectory x_c in a free space without force from the environment. That is to say that there is no interaction between the robot and its environment. Consequently, the simulation aim is to verify the effectiveness of the proposed control (29) without interaction between the robot and its environment. The parameters of the object are $m_o = 1$ kg, $g = 9.8$ m/s². The controller parameters are $k_1 = k_2 = k_3 = 50$, $K_2 = \text{diag}[70, 70, 70]$ and $K_r = \text{diag}[1, 1, 1]$. The updating law parameters are $\Gamma_G = \Gamma_C = \Gamma_M = \text{diag}[20, 20, 20]$, $\sigma_G = \sigma_C = \sigma_M = 0.01$. The frontier of the output constraint is $k_{c1} = 1.1 + 0.2 \sin(t)$, $k_{c2} = 1.01 + 0.2 \sin(t)$ and

$k_{c3} = 1.01 - 0.2 \cos(t)$. The parameters of the impedance model are $M_d = \text{diag}[0.1, 0.1, 0.1]$, $C_d = \text{diag}[5, 5, 5]$ and $G_d = [10, 10, 10]$.

The simulation results of case one are presented in Figs. 4-7. It can be known from Fig. 4 that two robots can carry the object along the desired trajectory x_c in a free space in desired accuracy. And Fig. 4 also shows that under the action of the proposed control (29), x_{1i} is constrained by time-varying constraint k_{ci} , given that initial conditions are constrained, $i = 1, 2, 3$. In Fig. 5, it is obvious that tracking error z_1 converges to a small value near zero. From the standpoint of tracking error z_1 , the tracking performance is also satisfactory. Fig. 6 shows control input F_o which is smooth and bounded. In Fig. 7, the motion of the object is plotted in Cartesian space, which illustrates that the tracking performance is satisfactory and the proposed control (29) has the ability to guarantee the output constraint. By analysing the above simulation results, it is known that the proposed control (29) can make the system output remain in the corresponding predefined constraint region.

Case two: In the second case, the wall is 0.8m away from the coordinate origin O along Z axis, therefore the coordinate of the wall is expressed as $(X = 0, Y = 0, Z = 0.8)$. For convenience, hereafter the location of the wall will be abbreviated as $Z = 0.8\text{m}$. The simulation procedure is that the object carried by two robots moves along the desired trajectory x_c from initial position to the wall ($Z = 0.8\text{m}$) in a free space and then after touching the wall, the object slides along the wall, finally leaves the wall and continues moving along the desired trajectory x_c in a free space. It should be emphasized that when the object touches the wall and then slides along it, the interaction between the robot and the wall develops. Consequently, the simulation aim is to verify the effectiveness of the proposed control (29) with interaction between the robot and the wall. The frontier of the output constraint is $k_{c1} = 1 + 0.1 \sin(t)$, $k_{c2} = 1.11 + 0.1 \sin(t)$ and $k_{c3} = 1.31 - 0.1 \cos(t)$. The rest of the parameters are the same as those of case one.

The simulation results of case two are presented in Figs. 8-11. It is known from Fig. 8 that the object moves along the the desired trajectory x_c , and slides along the wall when maintaining in contact with the wall. When the object slides along the wall, the target impedance is achieved, and the interaction force between the robot and the wall regulars the control input in order to improve this interaction. Fig. 8 also shows that corresponding time-varying constraint isn't violated. In Fig. 9, it is obvious that tracking error z_1 converges to a small value near zero. Fig. 10 shows the control input. It is noted that there are a few oscillations while the object comes in contact with the wall. This is due to the change in the unknown environment, but the control force tends immediately to be smooth by using the proposed control (29). In Fig. 11, it is seen that the object moves along the desired trajectory x_c from initial position to the wall, and after encountering the wall, the object slides along the wall, then continues moving to initial position along the desired trajectory x_c . Therefore, by analysing the simulation results, we know that the proposed control (29) with impedance learning and time-varying constraint can improve the environment-robot interaction better,

and make the system output remain in the corresponding time-varying constraint region.

B. Control Design with Full-State Constraint

Case three: In the three case, the simulation procedure is the same as that of case one. The simulation aim is to verify the effectiveness of the proposed control (53) without interaction between the robot and its environment. Controller parameters are $k_{11} = k_{12} = k_{13} = 20$. The frontier of the state constraint is $k_{d1} = k_{d2} = k_{d3} = 1.3 + 0.2 \cos(t)$. The rest of the parameters are the same as those of case one.

The simulation results of case three are presented in Figs. 12-16. It can be known from Fig. 12 that two robots can carry the object along the desired trajectory x_c in desired accuracy. And x_{1i} is constrained by time-varying constraint bound k_{ci} , $i = 1, 2, 3$. Fig. 13 shows tracking errors which converge to a small value near zero. Fig. 14 shows velocity variable x_{2i} which is constrained by time-varying constraint k_{di} , $i = 1, 2, 3$. Fig. 15 shows control input F_o which is smooth. Fig. 16 shows that actual movement trajectory x_1 converges to the desired trajectory x_c generated by impedance learning in a short period. Therefore, by analysing the simulation results, we know that the proposed control (53) with the full-state time-varying constraint can make the system states remain the corresponding predefined constraint region.

Case four: In the four case, the simulation procedure is the same as that of case two. The simulation aim is to verify the effectiveness of the proposed control (53) with interaction between the robot and its environment. Controller parameters are $k_{11} = k_{12} = k_{13} = 20$. The frontier of the state constraint is $k_{d1} = k_{d2} = k_{d3} = 1.3 + 0.2 \cos(t)$ and $k_{c1} = 1 + 0.1 \sin(t)$, $k_{c2} = 1.31 + 0.1 \sin(t)$, $k_{c3} = 1.31 - 0.1 \cos(t)$. The rest of the parameters are the same as those of case one.

The simulation results of case four are presented in Figs. 17-21. In Fig. 17, the object tracks the desired trajectory x_c , slides along the wall when maintaining contact in with the wall, and continues tracking the desired trajectory x_c after leaving the wall. In Fig. 18, it is obvious that tracking error z_1 converges to a small value near zero. Figs. 17 and 19 show that full-state constraint cannot be violated, which states that the proposed control (53) has the ability to guarantee the full-state constraint. Fig. 20 shows the control input. It is noted that there are a few oscillations while the object comes in contact with the wall. This is due to the change in the unknown environment, but the control force tends immediately to be smooth by using the proposed control (53). Fig. 21 gives the motion of the object in Cartesian space. Therefore, we know that the proposed control (53) with impedance learning and the full-state time-varying constraint can improve the environment-robot interaction better, and make the system states remain in the corresponding time-varying constraint region.

V. CONCLUSION

In this paper, an adaptive FNN control scheme is proposed for coordinated multiple robots with unknown dynamics and time-varying constraints using impedance learning. Two control design schemes are considered, respectively, for

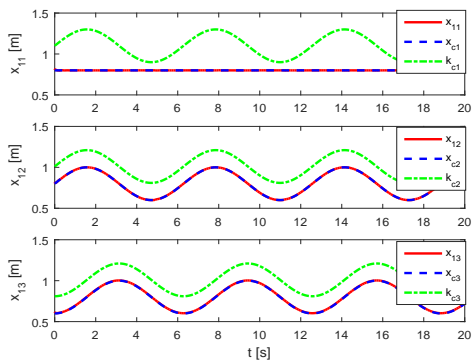


Fig. 4. Case one: Tracking performance

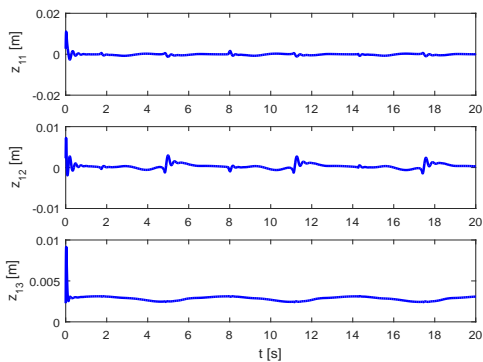


Fig. 5. Case one: Tracking error

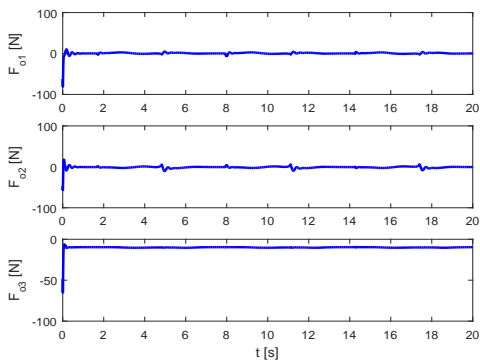


Fig. 6. Case one: Control input

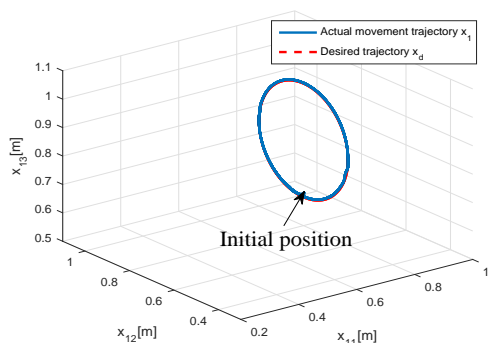


Fig. 7. Case one: The object's actual movement trajectory in Cartesian space

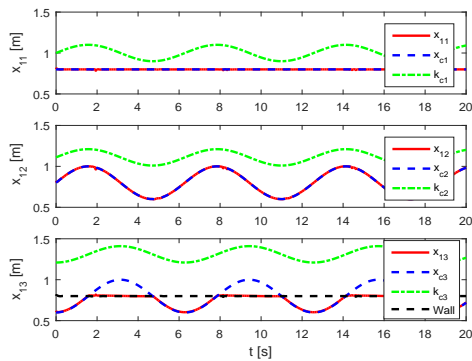


Fig. 8. Case two: Tracking performance

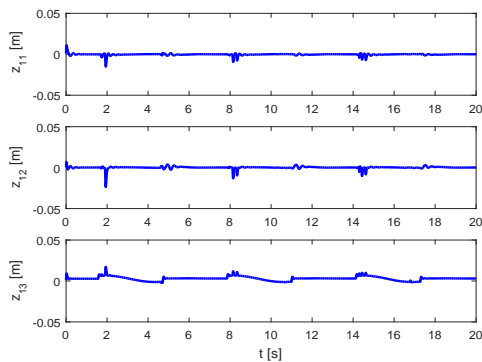


Fig. 9. Case two: Tracking error

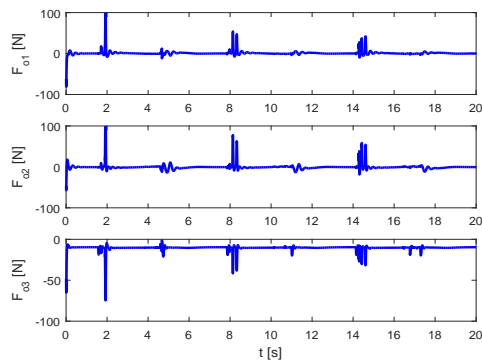


Fig. 10. Case two: Control input

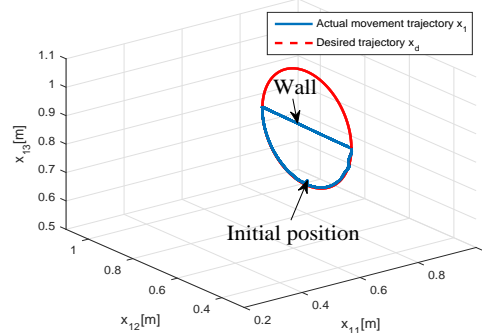


Fig. 11. Case two: The object's actual movement trajectory in Cartesian space

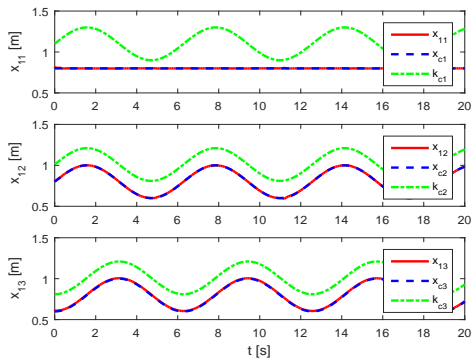


Fig. 12. Case three: Tracking performance

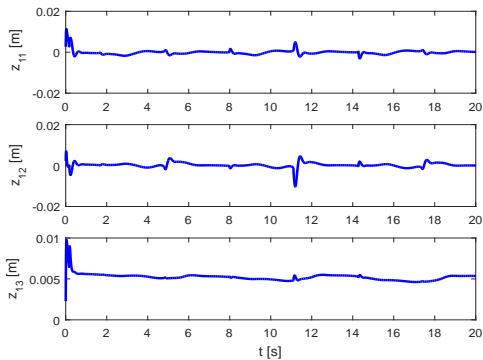


Fig. 13. Case three: Tracking error

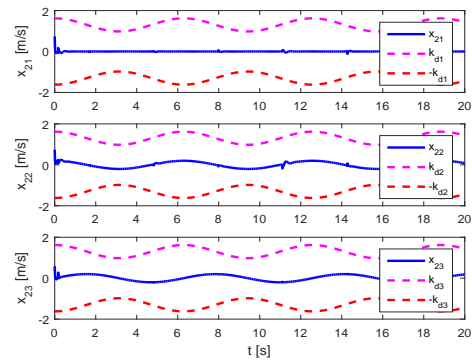


Fig. 14. Case three: Constrained velocity variable x_2

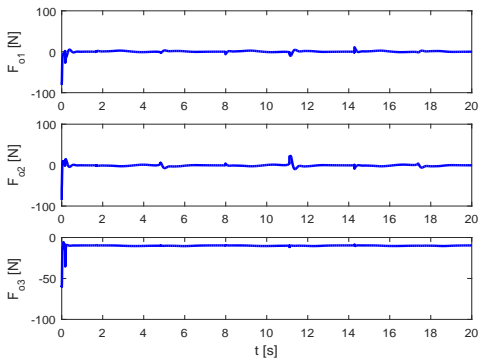


Fig. 15. Case three: Control input

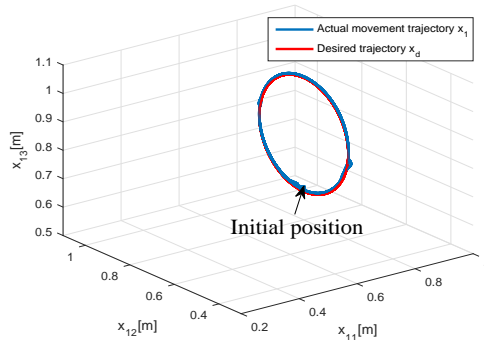


Fig. 16. Case three: The object's actual movement trajectory in Cartesian space

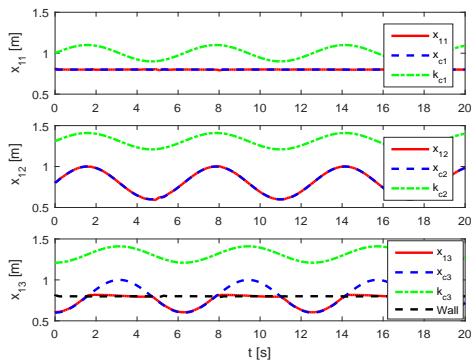


Fig. 17. Case four: Tracking performance

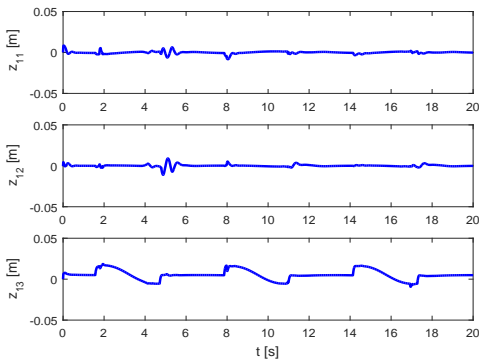


Fig. 18. Case four: Tracking error

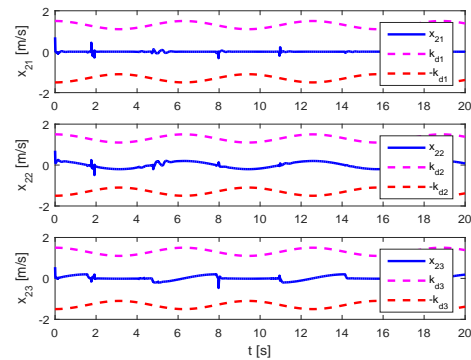


Fig. 19. Case four: Constrained velocity variable x_2

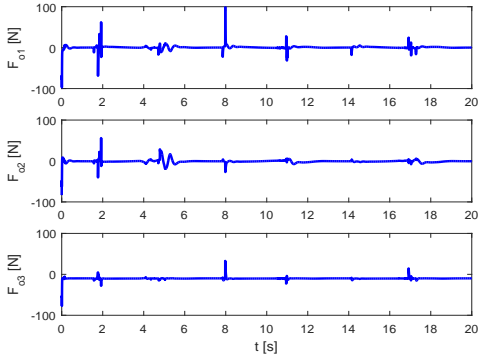


Fig. 20. Case four: Control input

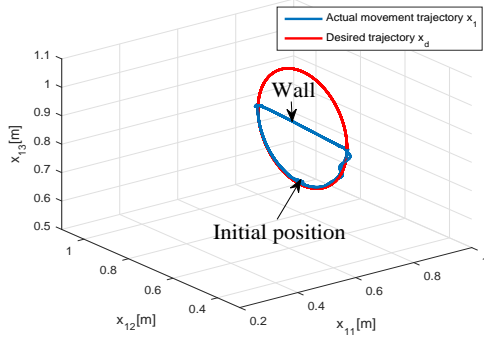


Fig. 21. Case four: The object's actual movement trajectory in Cartesian space

coordinated multiple robots: 1) Control design with output constraint. 2) Control design with full state constraint. FNNs are used to approximate the unknown dynamics. Integral Barrier Lyapunov function is introduced to avoid the violation of constraints. Impedance learning is employed to improve the environment-robot interaction. Four different simulations are carried out to verify the effectiveness of the proposed control. It is noted that there are a few oscillations happening in the control input while the robot comes in contact with the unknown environment. These oscillations maybe cause damage to the motor. The future research is to design a control scheme for restraining these oscillations.

ACKNOWLEDGEMENT

The authors would like to thank the Editor-In-Chief, the Associate Editor and the anonymous reviewers for their constructive comments which helped improve the quality and presentation of this paper.

APPENDIX

A. Proof of Remark 1

Step one: Let $g(z_i) = \int_0^{z_i} \frac{\sigma k_{ci}^2}{k_{ci}^2 - (\sigma + \alpha_i)^2} d\sigma - \frac{z_i^2}{2} = \int_0^{z_i} \frac{\sigma(\sigma + \alpha_i)^2}{k_{ci}^2 - (\sigma + \alpha_i)^2} d\sigma$. The derivative of $g(z_i)$ is $\dot{g}(z_i) = \frac{z_i x_i^2}{k_{ci}^2 - x_i^2}$ over the compact set $\omega := \{x_i ||x_i| < k_{ci}\}$, we have $k_{ci}^2 - x_i^2 > 0$.

Case one: $z_i < 0$, we have $\dot{g}(z_i) < 0$.

Case two: $z_i > 0$, we have $\dot{g}(z_i) > 0$.

Since $z_i = 0$, $g_{z_i} = 0$. Further, there is $g(z_i) > 0$ over the compact set $\omega := \{x_i ||x_i| < k_{ci}\}$. We have $\int_0^{z_i} \frac{\sigma k_{ci}^2}{k_{ci}^2 - (\sigma + \alpha_i)^2} d\sigma > \frac{z_i^2}{2}$.

Step two: Define $p_i(\sigma, \alpha_i) = \frac{\sigma k_{ci}^2}{k_{ci}^2 - (\sigma + \alpha_i)^2}$. It can be seen that $\frac{\partial p_i}{\partial \sigma} = \frac{k_{ci}^2 - \sigma^2 - \alpha_i^2}{k_{ci}^2 - (\sigma + \alpha_i)^2}$, which is positive over the compact set $|\sigma + \alpha_i| < k_{ci}$. Since $p_i(0, \alpha_i) = 0$ for $|\alpha_i| < k_{ci}$, and $p_i(\sigma, \alpha_i)$ is increasing with σ over the compact set $|\sigma + \alpha_i| < k_{ci}$, we further have $\int_0^{z_i} p_i(\sigma, \alpha_i) d\sigma \leq z_i p_i(\sigma, \alpha_i)$ for $|\sigma + \alpha_i| < k_{ci}$. We further obtain $\int_0^{z_i} \frac{\sigma k_{ci}^2}{k_{ci}^2 - (\sigma + \alpha_i)^2} d\sigma \leq \frac{k_{ci}^2 z_i^2}{k_{ci}^2 - x_i^2}$.

Combining Step one and Step two, the proof of Remark 1 is completed.

B. Proof of Theorem 1

Multiplying $e^{\kappa_3 t}$ in both sides of $\dot{V}_3 \leq -\kappa_3 V_3 + C_3$, there is $(V_3 + \kappa_3 V_3) e^{\kappa_3 t} \leq C_3 e^{\kappa_3 t}$. After integration, there is $V_3(t) \leq (V_3(0) - \frac{C_3}{\kappa_3}) e^{-\kappa_3 t} + \frac{C_3}{\kappa_3} \leq V_3(0) + \frac{C_3}{\kappa_3}$. Considering Remark 1, we easily know that $\frac{z_{1i}^2}{2} \leq \sum_{i=1}^n \frac{z_{1i}^2}{2} \leq \sum_{i=1}^n \int_0^{z_{1i}} \frac{\sigma k_{ci}^2}{k_{ci}^2 - (\sigma + \alpha_i)^2} d\sigma \leq V_3(0) + \frac{C_3}{\kappa_3}$. Further there are $|z_{1i}| \leq \sqrt{2B}$, $i = 1, \dots, n$, $\|z_2\| \leq \sqrt{\frac{2B}{\lambda_{\max}(M)}}$, where $B := V_3(0) + \frac{C_3}{\kappa_3}$.

C. Proof of Theorem 2

Since $\|\int_0^t g(\tau) N(z_2) \dot{z}_2 e^{\tau t} d\tau\| \leq \mathcal{N}$, we have $V_6(t) \leq V_6(0) + \frac{C_6}{\kappa_6} + \mathcal{N}$. Considering Lemma 1, we easily know that $\frac{z_{2i}^2}{2} \leq \sum_{i=1}^n \frac{z_{2i}^2}{2} \leq \sum_{i=1}^n \int_0^{z_{2i}} \frac{\sigma k_{ci}^2}{k_{ci}^2 - (\sigma + x_{di})^2} d\sigma \leq V_6(0) + \frac{C_6}{\kappa_6} + \mathcal{N}$ and $\frac{z_{1i}^2}{2} \leq \sum_{i=1}^n \frac{z_{1i}^2}{2} \leq \sum_{i=1}^n \int_0^{z_{1i}} \frac{\sigma k_{ci}^2}{k_{ci}^2 - (\sigma + \alpha_i)^2} d\sigma \leq V_6(0) + \frac{C_6}{\kappa_6} + \mathcal{N}$. Further there are $|z_{1i}| \leq \sqrt{2B_1}$ and $|z_{2i}| \leq \sqrt{2B_1}$, $i = 1, \dots, n$, where $B_1 := V_6(0) + \frac{C_6}{\kappa_6} + \mathcal{N}$.

REFERENCES

- [1] T. Noritsugu, T. Tanaka, and T. Yamanaka, "Application of rubber artificial muscle manipulator as a rehabilitation robot," in *Robot and Human Communication, 1996., 5th IEEE International Workshop on*, pp. 112–117, Nov 1996.
- [2] M. Browne, "Robots at work with medicines and adhesives," *Production Engineer*, vol. 64, pp. 19–20, September 1985.
- [3] M. Zhang, S. Q. Xie, X. Li, G. Zhu, W. Meng, X. Huang, and A. Veale, "Adaptive patient-cooperative control of a compliant ankle rehabilitation robot (carr) with enhanced training safety," *IEEE Transactions on Industrial Electronics*, vol. PP, no. 99, pp. 1–1, 2017.
- [4] Y. Bian, L. Zhao, H. Li, G. Yang, L. Geng, and X. Deng, "Research on multi-modal human-machine interface for aerospace robot," in *2015 7th International Conference on Intelligent Human-Machine Systems and Cybernetics*, vol. 1, pp. 535–538, Aug 2015.
- [5] M. Tognon and A. Franchi, "Dynamics, control, and estimation for aerial robots tethered by cables or bars," *IEEE Transactions on Robotics*, vol. 33, pp. 834–845, Aug 2017.
- [6] N. Wang and J. E. Meng, "Direct adaptive fuzzy tracking control of marine vehicles with fully unknown parametric dynamics and uncertainties," *IEEE Transactions on Control Systems Technology*, vol. 24, no. 5, pp. 1845–1852, 2016.
- [7] N. Wang, C. Qian, J. C. Sun, and Y. C. Liu, "Adaptive robust finite-time trajectory tracking control of fully actuated marine surface vehicles," *IEEE Transactions on Control Systems Technology*, vol. 24, no. 4, pp. 1454–1462, 2016.
- [8] Z. Li, J. Li, and Y. Kang, "Adaptive robust coordinated control of multiple mobile manipulators interacting with rigid environments," *Automatica*, vol. 46, no. 12, pp. 2028–2034, 2010.
- [9] W. He, S. S. Ge, Y. Li, E. Chew, and Y. S. Ng, "Neural network control of a rehabilitation robot by state and output feedback," *Journal of Intelligent & Robotic Systems*, vol. 80, no. 1, pp. 15–31, 2015.

- [10] M. Hamdy and G. El-Ghazaly, "Adaptive neural decentralized control for strict feedback nonlinear interconnected systems via backstepping," *Neural Computing & Applications*, vol. 24, no. 2, pp. 259–269, 2014.
- [11] Q. Yang, S. S. Ge, and Y. Sun, "Adaptive actuator fault tolerant control for uncertain nonlinear systems with multiple actuators," *Automatica*, vol. 60, pp. 92–99, Oct. 2015.
- [12] S. L. Dai, M. Wang, and C. Wang, "Neural learning control of marine surface vessels with guaranteed transient tracking performance," *IEEE Transactions on Industrial Electronics*, vol. 63, no. 3, pp. 1717–1727, 2016.
- [13] M. Wang and C. Wang, "Learning from adaptive neural dynamic surface control of strict-feedback systems," *IEEE Transactions on Neural Networks & Learning Systems*, vol. 26, no. 6, pp. 1247–1259, 2015.
- [14] D. Liu, D. Wang, and H. Li, "Decentralized stabilization for a class of continuous-time nonlinear interconnected systems using online learning optimal control approach," *IEEE Transactions on Neural Networks and Learning Systems*, vol. 25, pp. 418–428, Feb 2014.
- [15] D. Wang, D. Liu, H. Li, B. Luo, and H. Ma, "An approximate optimal control approach for robust stabilization of a class of discrete-time nonlinear systems with uncertainties," *IEEE Transactions on Systems Man & Cybernetics Systems*, vol. 46, no. 5, pp. 713–717, 2016.
- [16] Q. Yang, S. S. Ge, and Y. Sun, "Adaptive actuator fault tolerant control for uncertain nonlinear systems with multiple actuators," *Automatica*, vol. 60, pp. 92 – 99, 2015.
- [17] S.-C. Tong, Y.-M. Li, and H.-G. Zhang, "Adaptive Neural Network Decentralized Backstepping Output-feedback Control for Nonlinear Large-scale Systems With Time Delays," *IEEE Transactions on Neural Networks*, vol. 22, no. 7, pp. 1073–1086, 2011.
- [18] Z. Li, L. Ding, H. Gao, G. Duan, and C. Y. Su, "Trilateral teleoperation of adaptive fuzzy force/motion control for nonlinear teleoperators with communication random delays," *IEEE Transactions on Fuzzy Systems*, vol. 21, no. 4, pp. 610–624, 2013.
- [19] C. Yang, Z. Li, R. Cui, and B. Xu, "Neural network-based motion control of an underactuated wheeled inverted pendulum model," *IEEE Transactions on Neural Networks and Learning Systems*, vol. 25, no. 11, pp. 2004–2016, 2014.
- [20] H. Li, L. Bai, L. Wang, Q. Zhou, and H. Wang, "Adaptive neural control of uncertain nonstrict-feedback stochastic nonlinear systems with output constraint and unknown dead zone," *IEEE Transactions on Systems Man & Cybernetics Systems*, vol. 47, no. 8, pp. 2048–2059, 2017.
- [21] Y. J. Liu, J. Li, S. Tong, and C. L. P. Chen, "Neural network control-based adaptive learning design for nonlinear systems with full-state constraints," *IEEE Transactions on Neural Networks and Learning Systems*, vol. 27, pp. 1562–1571, July 2016.
- [22] Y. Song, X. Huang, and C. Wen, "Tracking control for a class of unknown nonsquare mimo nonaffine systems: A deep-rooted information based robust adaptive approach," *IEEE Transactions on Automatic Control*, vol. 61, no. 10, pp. 3227–3233, 2016.
- [23] C. L. P. Chen, G. X. Wen, Y. J. Liu, and Z. Liu, "Observer-based adaptive backstepping consensus tracking control for high-order nonlinear semi-strict-feedback multiagent systems," *IEEE Transactions on Cybernetics*, vol. 46, no. 7, pp. 1591–1601, 2016.
- [24] Y. H. Kim and F. L. Lewis, "Neural network output feedback control of robot manipulators," *IEEE Transactions on Robotics and Automation*, vol. 15, pp. 301–309, Apr 1999.
- [25] B. Xu, C. Yang, and Y. Pan, "Global neural dynamic surface tracking control of strict-feedback systems with application to hypersonic flight vehicle," *IEEE Transactions on Neural Networks and Learning Systems*, vol. 26, pp. 2563–2575, Oct 2015.
- [26] C. Yang, Y. Jiang, Z. Li, W. He, and C. Y. Su, "Neural control of bimanual robots with guaranteed global stability and motion precision," *IEEE Transactions on Industrial Informatics*, vol. 13, pp. 1162–1171, June 2017.
- [27] H. Li, Z. Chen, L. Wu, and H. K. Lam, "Event-triggered control for nonlinear systems under unreliable communication links," *IEEE Transactions on Fuzzy Systems*, vol. 25, pp. 813–824, Aug 2017.
- [28] Q. Zhou, H. Li, L. Wang, and R. Lu, "Prescribed performance observer-based adaptive fuzzy control for nonstrict-feedback stochastic nonlinear systems," *IEEE Transactions on Systems, Man, and Cybernetics: Systems*, vol. PP, no. 99, pp. 1–12, 2017.
- [29] L. Wang, M. Basin, H. Li, and R. Lu, "Observer-based composite adaptive fuzzy control for nonstrict-feedback systems with actuator failures," *IEEE Transactions on Fuzzy Systems*, vol. PP, no. 99, pp. 1–1, 2017.
- [30] H. A. Yousef, M. Hamdy, and K. Nashed, "L1 adaptive fuzzy controller for a class of nonlinear systems with unknown backlash-like hysteresis," *International Journal of Systems Science*, pp. 1–12, 2017.
- [31] M. Hamdy and G. El-Ghazaly, "Extended dynamic fuzzy logic system for a class of mimo nonlinear systems and its application to robotic manipulators," *Robotica*, vol. 31, no. 2, pp. 251–265, 2013.
- [32] J. Wang, A. B. Rad, and P. T. Chan, *Indirect adaptive fuzzy sliding mode control: Part I: fuzzy switching*. Elsevier North-Holland, Inc., 2001.
- [33] C.-Y. Su, M. Oya, and H. Hong, "Stable adaptive fuzzy control of nonlinear systems preceded by unknown backlash-like hysteresis," *IEEE Transactions on Fuzzy Systems*, vol. 11, pp. 1–8, Feb 2003.
- [34] Z. Liu, F. Wang, Y. Zhang, X. Chen, and C. L. Chen, "Adaptive fuzzy output-feedback controller design for nonlinear systems via backstepping and small-gain approach," *IEEE Transactions on Cybernetics*, vol. 44, no. 10, pp. 1714–1725, 2014.
- [35] X. Xie, D. Yang, and H. Ma, "Observer design of discrete-time t-s fuzzy systems via multi-instant homogenous matrix polynomials," *IEEE Transactions on Fuzzy Systems*, vol. 22, pp. 1714–1719, Dec 2014.
- [36] W. He and Y. Dong, "Adaptive fuzzy neural network control for a constrained robot using impedance learning," *IEEE Transactions on Neural Networks and Learning Systems*, vol. PP, no. 99, pp. 1–13, 2017.
- [37] M. Hamdy, S. Abd-Elhaleem, and M. A. Fkirin, "Time-varying delay compensation for a class of nonlinear control systems over network via h_∞ adaptive fuzzy controller," *IEEE Transactions on Systems, Man, and Cybernetics: Systems*, vol. 47, pp. 2114–2124, Aug 2017.
- [38] N. Wang and M. J. Er, "Direct adaptive fuzzy tracking control of marine vehicles with fully unknown parametric dynamics and uncertainties," *IEEE Transactions on Control Systems Technology*, vol. 24, pp. 1845–1852, Sept 2016.
- [39] H. Yang, X. Fan, P. Shi, and C. Hua, "Nonlinear control for tracking and obstacle avoidance of a wheeled mobile robot with nonholonomic constraint," *IEEE Transactions on Control Systems Technology*, vol. 24, no. 2, pp. 741–746, 2016.
- [40] Z. Zhang, S. Xu, and B. Zhang, "Asymptotic tracking control of uncertain nonlinear systems with unknown actuator nonlinearity," *IEEE Transactions on Automatic Control*, vol. 59, pp. 1336–1341, May 2014.
- [41] Z. Zhang, S. Xu, and B. Zhang, "Exact tracking control of nonlinear systems with time delays and dead-zone input," *Automatica*, vol. 52, pp. 272 – 276, 2015.
- [42] R. Cui, X. Zhang, and D. Cui, "Adaptive sliding-mode attitude control for autonomous underwater vehicles with input nonlinearities," *Ocean Engineering*, vol. 123, pp. 45–54, 2016.
- [43] S. Zhang, W. He, and D. Huang, "Active vibration control for a flexible string system with input backlash," *IET Control Theory & Applications*, vol. 10, no. 7, pp. 800–805, 2016.
- [44] C. Hua, L. Zhang, and X. Guan, "Distributed adaptive neural network output tracking of leader-following high-order stochastic nonlinear multi-agent systems with unknown dead-zone input," *IEEE Transactions on Cybernetics*, vol. 47, no. 1, pp. 177–185, 2017.
- [45] C. Hua, Y. Li, and X. Guan, "Finite/fixed-time stabilization for nonlinear interconnected systems with dead-zone input," *IEEE Transactions on Automatic Control*, vol. 62, no. 5, pp. 2554–2560, 2017.
- [46] W. He, T. Meng, S. Zhang, J. K. Liu, G. Li, and C. Sun, "Dual-loop adaptive iterative learning control for a timoshenko beam with output constraint and input backlash," *IEEE Transactions on Systems, Man, and Cybernetics: Systems*, vol. PP, no. 99, pp. 1–12, 2017.
- [47] H. Li, L. Bai, L. Wang, Q. Zhou, and H. Wang, "Adaptive neural control of uncertain nonstrict-feedback stochastic nonlinear systems with output constraint and unknown dead zone," *IEEE Transactions on Systems, Man, and Cybernetics: Systems*, vol. 47, pp. 2048–2059, Aug 2017.
- [48] X. He, W. He, J. Shi, and C. Sun, "Boundary vibration control of variable length crane systems in two-dimensional space with output constraints," *IEEE/ASME Transactions on Mechatronics*, vol. 22, pp. 1952–1962, Oct 2017.
- [49] Y. J. Liu, S. Lu, D. Li, and S. Tong, "Adaptive controller design-based ablf for a class of nonlinear time-varying state constraint systems," *IEEE Transactions on Systems, Man, and Cybernetics: Systems*, vol. 47, pp. 1546–1553, July 2017.
- [50] W. He, Y. Chen, and Z. Yin, "Adaptive neural network control of an uncertain robot with full-state constraints," *IEEE Transactions on Cybernetics*, vol. 46, pp. 620–629, March 2016.
- [51] M. A. Rami and D. Napp, "Discrete-time positive periodic systems with state and control constraints," *IEEE Transactions on Automatic Control*, vol. 61, pp. 234–239, Jan 2016.
- [52] Y. J. Liu and S. Tong, "Barrier lyapunov functions for nussbaum gain adaptive control of full state constrained nonlinear systems," *Automatica*, vol. 76, pp. 143–152, 2017.
- [53] Y. J. Liu and S. Tong, "Barrier lyapunov functions-based adaptive control for a class of nonlinear pure-feedback systems with full state constraints," *Automatica*, vol. 64, no. C, pp. 70–75, 2016.

- [54] Z. L. Tang, S. S. Ge, K. P. Tee, and W. He, "Robust adaptive neural tracking control for a class of perturbed uncertain nonlinear systems with state constraints," *IEEE Transactions on Systems Man & Cybernetics Systems*, pp. 1–12, 2016.
- [55] W. He, H. Huang, and S. S. Ge, "Adaptive neural network control of a robotic manipulator with time-varying output constraints," *IEEE Transactions on Cybernetics*, vol. 47, pp. 3136–3147, Oct 2017.
- [56] Z. L. Tang, S. S. Ge, K. P. Tee, and W. He, "Robust adaptive neural tracking control for a class of perturbed uncertain nonlinear systems with state constraints," *IEEE Transactions on Systems Man & Cybernetics Systems*, vol. 46, no. 12, pp. 1618–1629, 2016.
- [57] N. Hogan, "Impedance control: An approach to manipulation, part i - theory, part ii - implementation, part iii - applications," *Journal of Dynamic Systems Measurement & Control*, vol. 107, no. 1, 1985.
- [58] W. S. Lu and Q. H. Meng, "Impedance control with adaptation for robotic manipulations," *Robotics & Automation IEEE Transactions on*, vol. 7, no. 3, pp. 408–415, 1991.
- [59] F. Y. Wang and Y. Gao, "On frequency sensitivity and mode orthogonality of flexible robotic manipulators," *IEEE/CAA Journal of Automatica Sinica*, vol. 3, no. 4, pp. 394–397, 2016.
- [60] Y. Li and S. S. Ge, "Humancrobot collaboration based on motion intention estimation," *IEEE/ASME Transactions on Mechatronics*, vol. 19, no. 3, pp. 1007–1014, 2014.
- [61] Y. Li and S. S. Ge, "Force tracking control for motion synchronization in human-robot collaboration," *Robotica*, vol. 34, no. 6, pp. 1260–1281, 2016.
- [62] L.-X. Wang, *Adaptive fuzzy systems and control: design and stability analysis*. Prentice-Hall, Inc., 1994.
- [63] S. S. Ge, C. C. Hang, T. H. Lee, and T. Zhang, *Stable Adaptive Neural Network Control*. Boston, USA: Kluwer Academic, 2001.
- [64] K. P. Tee and S. S. Ge, "Control of state-constrained nonlinear systems using integral barrier lyapunov functionals," in *Decision and Control*, pp. 3239–3244, 2012.



Linghuan Kong received the B.Eng. degree from the College of Engineering, Qufu Normal University, Rizhao, China, in 2016 and the M.Eng. degree from the School of Automation Engineering, University of Electronic Science and Technology of China, Chengdu, China, in 2019. He is currently pursuing the Ph.D. degree with the School of Automation and Electrical Engineering, University of Science and Technology Beijing, Beijing, China.

His current research interests include robotics, neural network control, and adaptive control.

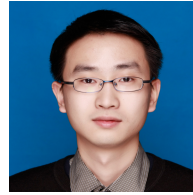


Wei He (S'09-M'12-SM'16) received his B.Eng. and his M.Eng. degrees from College of Automation Science and Engineering, South China University of Technology (SCUT), China, in 2006 and 2008, respectively, and his Ph.D. degree from Department of Electrical & Computer Engineering, the National University of Singapore (NUS), Singapore, in 2011.

He is currently working as a full professor in School of Automation and Electrical Engineering, University of Science and Technology Beijing, Beijing, China. He has co-authored 2 books published in

Springer and published over 100 international journal and conference papers. He was awarded a Newton Advanced Fellowship from the Royal Society, UK in 2017. He was a recipient of the IEEE SMC Society Andrew P. Sage Best Transactions Paper Award in 2017. He is serving the Chair of IEEE SMC Society Beijing Capital Region Chapter. He is serving as an Associate Editor of *IEEE Transactions on Neural Networks and Learning Systems*, *IEEE Transactions on Control Systems Technology*, *IEEE Transactions on Systems, Man, and Cybernetics: Systems*, *IEEE/CAA Journal of Automatica Sinica*, *Neurocomputing*, and an Editor of *Journal of Intelligent & Robotic Systems*.

His current research interests include robotics, distributed parameter systems and intelligent control systems.



Chenguang Yang (M'10-SM'16) received the B.Eng. degree in measurement and control from Northwestern Polytechnical University, Xian, China, in 2005, and the Ph.D. degree in control engineering from the National University of Singapore, Singapore, in 2010. He was a Post-Doctoral Fellow with Imperial College London, London, U.K. His current research interests include robotics and automation.

Dr. Yang was a recipient of the Best Paper Awards from the *IEEE TRANSACTIONS ON ROBOTICS* and a number of international conferences.



Zhijun Li (M'07-SM'09) received the Ph.D. degree in mechatronics, Shanghai Jiao Tong University, P. R. China, in 2002. From 2003 to 2005, he was a postdoctoral fellow in Department of Mechanical Engineering and Intelligent systems, The University of Electro-Communications, Tokyo, Japan. From 2005 to 2006, he was a research fellow in the Department of Electrical and Computer Engineering, National University of Singapore, and Nanyang Technological University, Singapore. Since 2012, he was a Professor in College of Automation Science

and Engineering, South China University of Technology, Guangzhou, China. From 2017, he is a Professor in Department of Automation, University of Science and Technology, Hefei, China.

From 2016, he has been the Co-Chairs of IEEE SMC Technical Committee on Bio-mechatronics and Bio-robotics Systems (B^2S), and IEEE-RAS Technical Committee on Neuro-Robotics Systems. He is serving as an Editor-at-large of *Journal of Intelligent & Robotic Systems*, and Associate Editors of several IEEE Transactions.

Dr. Li's current research interests include wearable robotics, tele-operation systems, nonlinear control, neural network optimization, etc.



Changyin Sun is the distinguished professor of the School of Automation, Southeast University and University of Science and Technology Beijing, both in China. He received his MS and PhD degrees in Electrical Engineering from the Southeast University, Nanjing, China, respectively, in 2001 and 2003. His research interests include intelligent control, flight control, pattern recognition, optimal theory, etc.